PRECODED DUAL-POLARIZED SPATIAL MODULATION OVER CORRELATED FADING CHANNELS

by

Negin Kazemipourleilabadi

B.S., Electrical and Electronic Engineering, University of Tabriz, 2014

Submitted to the Institute for Graduate Studies in
Science and Engineering in partial fulfillment of
the requirements for the degree of
Master of Science

Graduate Program in Electrical and Electronics Engineering
Boğaziçi University

2018

ACKNOWLEDGEMENTS

I would first like to express my most sincere gratitude to my thesis advisor, Prof. Mutlu Koca. He was always encouraging my research and his advices on my researches was very valuable. His office door was always open whenever I had a problem or question about my research, and without a doubt this work would not have been present without his support and guidance. I would also like to thank my committee members, Prof. Emin Anarım and Assoc. Prof. Ertuğrul Başar, for their valuable comments and profound knowledge.

My special thanks goes to my family for all their love, understanding and encouragement. They were always been my truest supporters. I can't find the words to express how grateful I am to my mother and father for their sacrifices they have made on my behalf.

Last but not least, I would like to thank all my friends, especially WCL's people, who supported me toward my goal and they made the time in lab very enjoyable.

ABSTRACT

PRECODED DUAL-POLARIZED SPATIAL MODULATION OVER CORRELATED FADING CHANNELS

In wireless communication systems, multiple-input multiple-output (MIMO) systems have been emerged and widely used during past decades to achieve higher data rates, better quality of service and higher network capacity. However, using multiple antennas results in an inevitable problem which is known as inter-channel interference. This is not the only issue due to the usage of multi-antennas, but also spatial correlation, which is the result of insufficient spacing among antennas. These effects deteriorate the performance of the system. Spatial modulation (SM) and using dual-polarizated (DP) antennas are introduced in MIMO systems to combat with the proposed problems respectively. In addition the joint utilization of both the antenna and signal spaces to convey information in SM causes a main drawback, specifically, if there is a direct line-of-sight (LOS) channel component (i.e., Rician fading) and/or spatial correlation among transmit antennas. This causes a significant degradation in the performance of the receiver in resolving the active transmit antenna and results in a large increase in the overall average bit-error rate performance of the DP-SM system. In this work, we address the effects of precoding for dual-polarized antennas over MIMO systems employing SM. This approach is based on phase-rotation of the transmitted symbols according to the active transmit antenna. The optimum values of the precoding coefficients are determined so as to minimize the asymptotic average bit-error rate. It is shown that there is a high performance improvement even in the case of heavily correlated transmit antennas and Rician channels in comparison to conventional DP-SM systems, and precoded uni-polarized SM systems.Later on, the results are extended to the case where the receiver estimates the channel imperfectly.

ÖZET

ÖN KODLAMALI ÇİFT-KUTUPSAL UZAMSAL KİPLENİM SİSTEMLERİN İLİNTİLİ SÖNÜLÜMLÜ KANALLARDA PERFORMANS ANALİZİ

Kablosuz iletişim sistemlerinden, çok-girdili çok-çıktılı (MIMO) sistemler daha yüksek veri hızı, daha iyi hizmet kalitesi ve yüksek şebeke kapasitesi sağladığı icin son yıllarda ortaya çıkmış ve yaygın olarak kullanılmıştır. Öte yandan, çok anten kullanımının neden olduğu, kanallar arası girişim olarak bilinen kaçınılmaz bir sorun vardır. Yalnızca kanallar-arası girişim degil, aynı zamanda bir başka sorun da antenler arası aralığın sonucu olan ilinti olarak bilinmektedir. Bu etkenler sistemin performansını düşürmektedir. Çok-girdili çok-çıktılı (MIMO) sistemlerde Uzamsal kiplenim ve çift-kutupsal (DP) antenleri kullanmak fikri bu sorunlarla mücadele etmek icin ortaya çıktı. Ayrıca uzamsal kiplenimde anten ve sinyal uzamlarının aynı anda kullanımı, özellikle Rician sönümleme etkisi ve verici antenler arasında olan uzamsal ilinti nedeni ile alıcı'nın performansını düşürmekte ve sonuç olarak ortalama bit hata oranını arttırmaktadır. Bu çalışmada ön kodlamalı cift-kutupsal uzamsal kiplenim sisteminin etkilerini hedef alıyoruz. Bu yaklaşım gönderilen sembollerin aktif verici antene göre faz-döndürme tekniğine dayalıdır. Ön kodlamadaki optimum faz-döndürme değerleri asimptotik ortalama bit hata oranını minimize eden değerlerle belirlenmektedir. Sonuçlara bakıldığında, ön kodlama yönteminin ağır ilinti ve Rician kanallarında ayni spektral verimliliğe sahip geleneksel çift-kutupsal antenli uzamsal kiplenim sistemine ve ön kodlamalı tek-kutupsal antenleri kullanarak uygulanan uzamsal kiplenim sistemine nazaran daha iyi performans sergilediği görülmektedir. Daha sonra, sonuçlar kanal kestirim hatasının olduğu durumlar için genişletilmiştir.

TABLE OF CONTENTS

LIST OF FIGURES

LIST OF TABLES

LIST OF SYMBOLS

a_{ij}	Description of a_{ij}
$\mathcal{CN}(m_x, {\sigma_x}^2)$	Complex Gaussian random variable with mean m_x and variance ${\sigma_x}^2$
$D(.)$	Distance metric
$E\{.\}$	Expectation operator
$\mathbf{G}$	Channel matrix for erroneous estimation
$\mathbf{g}_u$	uth column of $\mathbf{G}$
$\mathbf{H}$	Channel matrix
$\overline{\overline{\mathbf{H}}}$	Deterministic matrix with all one elements
$\bar{\mathbf{H}}_w$	Fixed part of the channel $\mathbf{H}$
$\tilde{\mathbf{H}}_w$	Variable part of the channel $\mathbf{H}$
$\mathbf{h}_u$	uth column of $\mathbf{H}$
$h_{i,j}$	Channel coefficient between ith receive antenna and jth transmit antenna
$I_0(.)$	Modified Bessel function of the first kind
K	Rician factor
L	L-ary digital modulation
ℓ	Number of bits assigned to constellation symbols
M	Number of transmit antennas
m	Number of bits assigned to antenna selection
N	number of receive antennas
$\mathbf{n}$	Noise vector
N_0	Variance of the noise
$\mathcal{N}(m_x, {\sigma_x}^2)$	Gaussian random variable with mean m_x and variance ${\sigma_x}^2$
P_r	Average received power
$\mathbf{R}_r$	Receive rotation matrix
$\mathbf{R}_t$	Transmit rotation matrix
R	Spectral efficiency
$\mathrm{Re}\{x\}$	Real part of a complex variable
$vec(.)$	Vectorization of a matrix
X	Transmitted symbol

$\mathbf{x}$	Transmitted signal
$\mathbf{y}$	Received signal
α_r	Spatial correlation coefficient at the receiver
α_t	Spatial correlation coefficient at the transmitter
χ_f	The ratio of co-polar to cross-polar term for fixed part of the channel
χ_v	The ratio of co-polar to cross-polar term for variable part of the channel
η	Signal to noise ratio (SNR)
$\mathbf{\Gamma}_f$	Leakage matrix for fixed part of the channel
$\mathbf{\Gamma}_v$	Leakage matrix for variable part of the channel
γ_r	Polarization correlation coefficient at the receiver
γ_t	Polarization correlation coefficient at the transmitter
$\mho$	Estimation error matrix
μ_f	Power leakage amount from one polarization to its orthogonal counterpart for fixed part the channel
μ_v	Power leakage amount from one polarization to its orthogonal counterpart for variable part the channel
$\mathbf{\Pi}_t$	Polarization correlation matrix at the transmitter
$\mathbf{\Pi}_r$	Polarization correlation matrix at the receiver
$\mathbf{\Psi}$	Diagonal precoding matrix
$\psi_{i,j}$	i,jth element of the precoding matrix
σ_e^2	Variance of the channel estimation error
$\sigma_{i,j}^r$	i,jth element of receive spatial correlation matrix
$\sigma_{i,j}^t$	i,jth element of transmit spatial correlation matrix
θ_r	Rotation angle relative to vertical direction at the receive side
θ_t	Rotation angle relative to vertical direction at the transmit side
θ_u	Rotation of the symbols transmitted from uth unique active transmit antenna and polarization pair
Φ_{r}	Receive correlation matrix
Φ_{t}	Transmit correlation matrix
$\mathbf{\Xi}_r$	Correlation matrix of the channel estimation error at the receiver

$\mathbf{\Xi}_t$	Correlation matrix of the channel estimation error at the transmitter
$\{.\}^*$	Complex conjugation
$\|.\|$	Determinant of a matrix
$\{.\}^\dagger$	Transposition of a matrix followed by conjugation
$\{.\}^H$	Hermitian of a matrix
$\{.\}^T$	Transpose of a matrix
$\odot$	Element by element Hadamard multiplication
$\otimes$	Kronecker product

LIST OF ACRONYMS/ABBREVIATIONS

ABEP	Average Bit Error Probability
APEP	Average Pairwise Error Probability
AWGN	Additive White Gaussian Noise
BER	Bit Error Probability
BICM	Bit-Interleaved Coded Modulation
bpcu	Bit per Channel Use
CSI	Channel State Information
C-SM	Conventional Spatial Modulation
DP	dual-polarized
exp	Exponential Function
G-SM	Generalized Spatial Modulation
i.i.d	Independent and Identically Distributed
ICI	Inter Channel Interference
LOS	Line of Sight
MGF	Moment Generating Function
MIMO	Multiple Input Multiple Output
ML	Maximum Likelihood
NLOS	Non Line of Sight
PDF	Probability Density Function
PEP	Pairwise Error Probability
SISO	Single Input Single Output
SM	Spatial Modulation
SMX	Spatial Multiplexing
SNR	Signal to Noise Ratio
STBC	Space-Time Block Coding
TITO	Two Input Two Output
UP	Uni Polarized
VH	Vertical-Horizontal
XPC	Polarization Correlation
XPD	Cross-Polar Discrimination

XPI	Cross-Polar Interference

1. INTRODUCTION

1.1. MIMO Communication

Wireless communication technology is facing a number of challenges, including the requirement of better data rates, higher capacity and improved service performance. Multiple-input multiple-output (MIMO) communication is an emerging technology to solve these measures. MIMO system which can be defined as using multiple antennas at both transmitting and receiving ends provides an additional spatial dimension for communication and yields a degree-of-freedom gain which results in an increase in the capacity. In addition high reliability and data rate arise from the use of the new dimension. Existence of multiple antennas in a system, means existence of different propagation paths. When multiple copies of the same data are sent from different active antennas they may experience different amounts of fading. Thus the chance of properly receiving the transmitted data increases. This improves the reliability of the system and is called spatial diversity or diversity gain. The second type of gain introduced in MIMO systems is multiplexing gain which comes from transmitting independent information symbols by different active antennas such as V-BLAST [1]. The multiplexing gain is also referred as degrees of freedom with reference to signal space constellation. Consequently, data rate is increased proportionally to the minimum number of transmitter and receiver without increasing the spectrum or transmit power. Today MIMO, which is also known as space-time wireless or smart antennas, is a breakthrough for mostly used and many newly emerged technologies, such as wireless local area networks (WLAN), third generation networks [2] and it has been penetrated to several wireless communication standards such as IEEE 802.11, HSPDA and LTE [3].

1.2. Spatial Modulation

Spatial modulation (SM) as in [4], [5], is a recently emerged and widely used transmission technology for MIMO communication systems. The main limitation of MIMO systems is related to their implementation complexity, which increases with the number of antennas. SM not only offers significant complexity reductions especially on the receiver side, but also provides better multiplexing gains (in some cases also diversity gain) in comparison to other MIMO technologies with the same spectral efficiency. The fundamental principle of SM is simple: The information is transmitted not only through the signal space via digital modulation but also through the antenna space. In this technique the bits of information are separated in two groups, the first group is used to activate a single transmit antenna, and the second part is used to choose a from the employed constellation. In conventional SM (C-SM) design, where there is just one active antenna at the transmitter side, inter channel interference (ICI) is avoided completely and it reduces the receiver complexity in comparison to other Spatial Multiplexing techniques such as the vertical Bell-Labs layered space-time coding (V-BLAST) approach [6]. C-SM is a specific model for the generalized SM (G-SM) shown in [7–10], in which the first portion of the transmitted bits is utilized to activate a group of transmit antennas simultaneously. The improved error performance especially for large spectral efficiencies in SM systems is the result of the increase in minimum distance between constellation points since spatial modulation assigns a number of information bits for the activated antenna index instead of allocating all bits to the constellation symbols, so the constellation size decreases comparing to other MIMO scenarios. A special case of G-SM is also presented in [11], where the advantages of G-SM are combined with the Alamouti space-time block coding (STBC) for enhanced error performance over C-SM and other spatial multiplexing techniques. In G-SM the same symbols might be transmitted from the active antennas and achieve diversity gain or different symbols might be transmitted from each active antenna and thus multiplexing gain is achieved as described before.

In general because of the rate improvements, implementation simplicity and performance enhancements, SM based wireless communication systems became a commonly used and as an interested research area in late years.

1.3. Dual-Polarized Spatial Modulation System

The performance of the SM-MIMO system is highly dependent on MIMO channel characteristics, which depends on antenna height, spacing and richness of the scattering. Generally, large antenna spacings are required to achieve significant multiplexing or diversity gains. SM-MIMO systems suffer from the physical space limitations to place multiple transmit and receive antennas. Uni-polarized (UP) antennas which have been used widely in previous SM-MIMO systems, need larger separation among antennas to decrease the impairments coming from correlation. Using dual-polarized antennas (polarization diversity) is a costly and spatially effective method, where two uni-polarized antennas are replaced by a single antenna employing orthogonal polarizations. It has been shown that orthogonal polarizations separate channels better, by imposing a higher decorrelation at receiver and transmitter sides of the wireless system. Moreover, in the correlated channels, DP-SM systems are more prominent in mild BER levels and in error floor, and these systems combat against the impairments coming from channel estimation errors. This is the reason why we add the polarization dimension to the signal and space dimensions. Ideally, all cross-polar transmissions which is described as a transmission from a vertical polarization of transmit antenna to an horizontal polarization of receive antenna (or vice versa) must equal to zero. But in the practical cases it is not zero and it results in two depolarization mechanisms : Antenna depolarization and scatterer-based depolarization. Both effects combines to yield a global cross-polar discrimination (XPD). Some evaluations have presented the relationship between cross-polar discrimination and the space between the receiver and the transmitter in [12], [13]. In [14] and [15], the effects of antenna configurations and propagation environments have been investigated, and it is shown that dual-polarized antennas provide uncorrelated branches and enhance the performance. Capacity of dual-polarized systems is investigated and compared with uni-polarized MIMO channels and the results prove that dual-polarized systems outperform uni-polarized ones in the conditions are non-ideal as in [14] and [16]. So application of spatial modulation using dual-polarized antennas as in [17], shows that the proposed architecture offers major performance benefits in comparison to UP systems with equal antenna numbers, also it's performance is near to the equivalent UP system where this system utilizes twice as much space to place antennas. Also from the results which are shown in [17],

it is obvious, dual-polarized spatial modulation systems are more resistant toward the corruptions such as spatial correlations and Rician fading effects in addition to errors coming from the estimation of the channel in comparison to uni-polarized spatial modulation, UP-SMX also DP-SMX [18] systems.

1.4. Precoded Dual-Polarized Spatial Modulation System

SM system operating with dual-polarized antennas is based on the utilization of antenna, polarization and signal spaces to transmit the information bits. This makes the overall average bit-error rate (ABER) to grow to higher values, especially, when the channel experiences Rician fading (i.e., direct line-of-sight component) and also when the antennas are correlated due to insufficient separation. At the transmitter, a major MIMO processing level is precoding. Precoding is a method that makes use of the information about channel which is present at the transmitter and improves the performance of the system. The design of the precoding for MIMO systems has become interested study field in last years and it has new applications in recently emerged wireless standards.

Different solutions has been introduced in previous works to get robustness against transmit correlation and line-of-sight component to improve the performance. For example in [19], [20] and [21], some kinds of protection for unequal error vulnerability are shown. Also trellis-coding based method in [22] is shown to provide robustness against aforementioned problems. However, in all of these works, the addition of an encoding-decoding couples results in latency and complexity of the system. Another line of work in [23–25] are presented, where in the presented approaches the precoding design is such that to form the observed constellation at the receiver in order to make the minimum Euclidean distance grow and decrease the bit-error probability. These precoding schemes are proposed just for time-invariant channels and for cases with the availability of full channel information at the transmitter. For this reason, throughout the thesis an extended precoding with shaping the constellation for time-variant fading channels with correlation effects at both ends of the system is considered, and we show a precoding technique which is more efficient in expense and difficulty, for enhanced stability against both adverse channel effects. A similar precoding approach has been

done for uni-polarized spatial modulation MIMO systems over correlated fading channels in [26]. Dissimilar to the approaches shown in [23–25], just the fixed part of the channel and the correlation coefficients are required at the transmitter. The introduced methodology is based on embarking several complex multiplying coefficients on the symbols transmitted and it preserves the no-ICI property because there is only one active antenna and also one active polarization direction. Additionally, it saves the average power consumption, and only an increase in the transmitter circuitry is required. The precoding operation is done by rotation of the constellations based on the active polarization of the active antenna.

1.5. Scope Of The Thesis

The main contribution of the presented work is to combine precoding and DP-SM system to make the system more robust toward both spatial correlations between transmit antennas and also Rician fading effects. The proposed technology which is established on the rotation for the transmitted symbol phases based on the activated transmitter antenna. The average power budget can be kept unchanged and there is no need for the channel state information to be fully known at the transmitter. The optimal values for the rotation of phases of the precoder matrix can be identified based on the minimization of the ABER (average bit-error rate) at asymptotically high SNR values. The precoded DP-SM scheme offers performances which are comparable to or under certain conditions even better than those of the precoded uni-polarized systems with the same spectral efficiency while using half as much space. Also the benefits of the precoding is demonstrated over high order systems and modulations, which increases the complexity of the ABER minimizing design. The theoretical error analysis is also extended to the case where the channel coefficients are estimated with Gaussian estimation errors. Theoretical formulations are also confirmed by wide simulations, both theoretical and simulation results illustrate high performance improvements particularly when the correlation between antennas is high in addition to LOS component over conventional DP-SM with a minor increment in the application difficulty at the transmitter. Also it is presented the need for unequal error protection is reduced for the precoded system in comparison to the conventional system.

1.6. Thesis Outline

The rest of the thesis is organized as follows: We review some background information introduced in Chapter 1, such as MIMO communication, spatial modulation, dual-polarized SM systems and precoding. Chapter 2, represents MIMO communication systems over different channel realizations. Spatial modulation is also introduced in this chapter as a new technology which can be implemented over MIMO systems. Chapter 3, describes dual-polarized antennas and their models in SISO and MIMO systems. also, dual-polarized spatial modulation systems is described in this chapter. Chapter 4, illustrates precoding approach for dual-polarized spatial modulation systems. The main contribution of this work is presented in this chapter, where the system model and the detection methodology and the precoder optimization are shown. Also ABER is computed for precoding scheme and the analysis of the precoding approach is described in perfect and erroneous channel estimation scenarios. The unequal error protection of the precoding scheme is shown in this chapter also. The simulation results for different channel cases are shown in chapter 4. Finally the conclusion part comes in Chapter 5.

2. FUNDAMENTALS OF MIMO AND SPATIAL MODULATION

The popularity of using MIMO systems in wireless communication has grown in past years for their abilities to improve the performance. The impairment of the signal in communication channels due to fading, affects the quality of the service and decreases the reliability of the system. Also the limited power and frequency bandwidth had forced the designers to work for higher data rates and more reliable systems. MIMO is an important technology in the design of wireless communication systems. It presents various advantages which can be solutions for both mentioned deteriorations in the channel in addition to source limitations. In addition to the single-input single-output (SISO) systems which are using time and frequency dimensions, MIMO system exploits the space dimension (ensuring the utilization of multiple transmit and receive antennas). The benefits of MIMO technology are: array gain, spatial multiplexing gain, spatial diversity gain and interference reduction. Figure **??**.1 shows a fundamental block diagram of a MIMO system. Information bits are encoded and interleaved first, then they are mapped to data symbols (such as QAM) by the symbol mapper. These data symbols are the inputs of space-time encoder, which outputs spatial data streams. These streams are mapped to transmit antennas by space-time precoding block. The signals propagate through the channel and arrive at the receiver antenna array. The receiver collects the signal and reverse all the transmitter operations in order to decode the data.

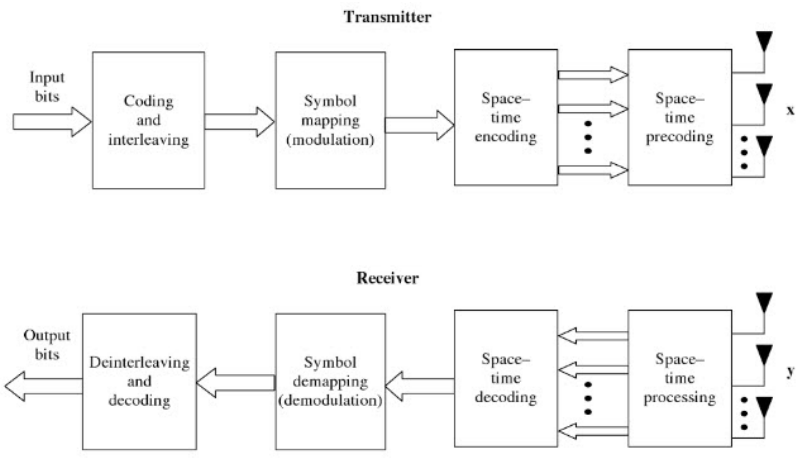

Figure 2.1. Block diagram for MIMO system.

2.1. MIMO Channel Model

For a system with N_T transmit antennas and N_R receive antennas, the MIMO channel matrix which is shown in figure 2.2 can be represented by a $N_R \times N_T$ matrix.

$$\mathbf{H} = \begin{bmatrix} h_{1,1} & h_{1,2} & \cdots & h_{1,(N_T)} \\ h_{2,1} & h_{2,2} & \cdots & h_{2,(N_T)} \\ h_{3,1} & h_{3,2} & \cdots & h_{3,(N_T)} \\ h_{4,1} & h_{4,2} & \cdots & h_{4,(N_T)} \\ \vdots & \vdots & \vdots & \vdots \\ h_{(N_R-1),1} & h_{(N_R-1),2} & \cdots & h_{(N_R-1),(N_T)} \\ h_{(N_R),1} & h_{(N_R),2} & \cdots & h_{(N_R),(N_T)} \end{bmatrix} \tag{2.1}$$

where $h_{n,m}$ is the channel gain between the $n-th$ receive and $m-th$ transmit antenna pair, where $n = 1, \ldots, N_R$ and $m = 1, \ldots, N_T$. Similar to the single-input single-output (SISO) system, the singular channel gains in the MIMO channel are usually modeled as circularly symmetric complex Gaussian random variables with zero-mean, consequently the envelope $|h_{n,m}|$ has the Rayleigh distribution as: (where z is assumed as the envelope of the channel gains)

$$p_Z(z) = \frac{z}{\sigma^2} \exp(\frac{-z^2}{2\sigma^2}) \tag{2.2}$$

and power $|h_{n,m}|^2$ are exponentially distributed.

In order to determine the spatial correlation coefficients let us assume a two-input two-output (TITO) system with the channel matrix defined as:

$$\mathbf{H} = \begin{bmatrix} h_{1,1} & h_{1,2} \\ h_{2,1} & h_{2,2} \end{bmatrix} \tag{2.3}$$

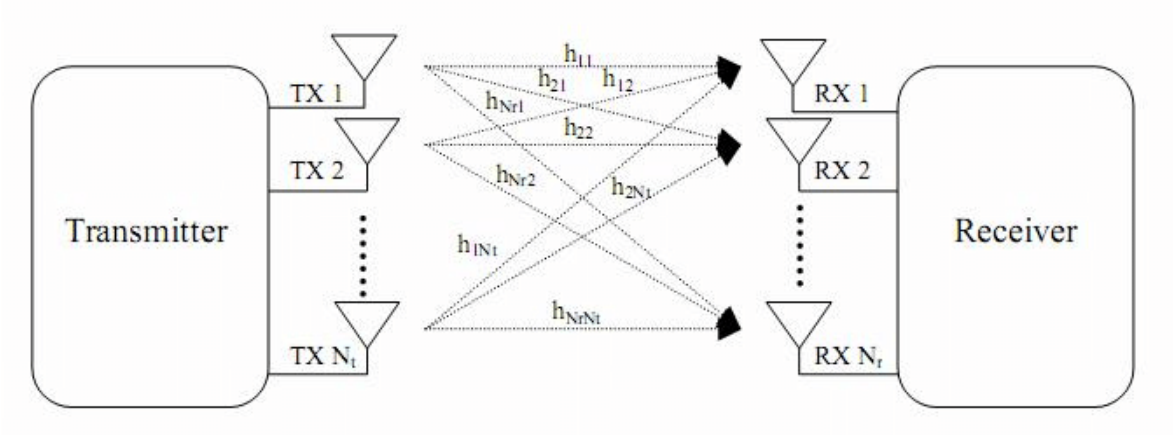

Figure 2.2. MIMO channel with N_T transmit and N_R receive antennas.

The transmit and receive spatial correlation coefficients are shown below respectively as:

$$E\left\{h_{1,1}{h_{1,2}}^*\right\} = E\left\{{h_{2,1}}^* h_{2,2}\right\} = \alpha_t,$$
$$E\left\{h_{1,1}{h_{2,1}}^*\right\} = E\left\{{h_{1,2}}^* h_{2,2}\right\} = \alpha_r \tag{2.4}$$

These effects can be collected in spatial correlation matrices $\mathbf{\Sigma_t}$ and $\mathbf{\Sigma_r}$ as:

$$\mathbf{\Sigma}_{\mathrm{t}} = \begin{bmatrix} 1 & \alpha_t \\ \alpha_t^* & 1 \end{bmatrix}, \qquad \mathbf{\Sigma}_{\mathrm{r}} = \begin{bmatrix} 1 & \alpha_r \\ \alpha_r^* & 1 \end{bmatrix} \tag{2.5}$$

This model can be extended to the $N_T \times N_R$ system, such that $\mathbf{\Sigma_t}$ and $\mathbf{\Sigma_r}$ are $N_T \times N_T$ transmitter and $N_R \times N_R$ receiver matrices of correlation, in order, due to the inter-antenna spacing and they can be defined as:

$$E\left\{\sum_k \mathbf{H_{i,k}} \mathbf{H_{j,k}^*}\right\} = [\mathbf{\Sigma_r}]_{i,j} = \sigma_{i,j}^r = \alpha_r^{|i-j|} \tag{2.6}$$

$$E\left\{\sum_k \mathbf{H_{k,i}} \mathbf{H_{k,j}^*}\right\} = [\mathbf{\Sigma_t}]_{i,j} = \sigma_{i,j}^t = \alpha_t^{|i-j|} \tag{2.7}$$

In practice it is reasonable to have more correlation for the nearest antennas and as the distance among antennas increases, the correlation decreases. By using the well known Kronecker model in [27] the channel matrix will become as

$$\mathbf{H} = \mathbf{\Sigma_r^{\frac{1}{2}}} \tilde{\mathbf{H}} \mathbf{\Sigma_t^{\frac{1}{2}T}} \tag{2.8}$$

where $\tilde{\mathbf{H}}$ is an $N_R \times N_T$ matrix whose elements are formed by Rayleigh distribution.

2.1.1. Independent and identically distributed (i.i.d) Rayleigh fading channel model

The correlation between individual antennas and channel gains in MIMO channel is a complicated function of the scattering environment and spacing at the transmitter and receiver. For example, an extreme case is when all antennas are collocated at the transmitter and receiver. In this case, all elements of $\mathbf{H}$ will be fully correlated and spatial diversity order of the channel equals 1. By increasing the space among antennas de-correlation of the channel elements will increase. But we have to notice that the antenna spacing does not ensure the de-correlation by itself. The combination of adequate antenna spacing with rich scattering in the environment ensures de-correlation of the MIMO channel elements. If the channel has rich scattering, the required antenna spacing is $\lambda/2$, where λ is the wavelength of the operation frequency. When the channel elements are perfectly decorrelated (the ideal conditions), $h_{n,m}(n = 1, \ldots, N_R, m = 1, \ldots, N_T) \sim \mathcal{CN}(0, 1)$ (complex-valued random variables with mean zero and variance 1). In these conditions $\mathbf{H} = \tilde{\mathbf{H}}$ is the independent and identically distributed frequency flat Rayleigh fading channel model.

2.1.2. Frequency-selective and time-selective fading

For the model of the channel in the previous part, we assumed that the product of the bandwidth and the delay spread is very small. With increasing one of these characteristics of the channel, the product is no longer negligible and it results in frequency-dependent channel realizations, i.e., $\mathbf{H}(\mathbf{f})$. The characteristics of the correlation in frequency domain are dependent on the power lateness side view. The minimum

required separation in bandwidth to achieve decorrelation is coherence bandwidth $\mathbf{B_c}$, and it is inversely proportional to the delay spread of the channel. Furthermore due to the motion of the scatterers in the environment, transmitter or receiver, the channel realizations will vary with time. The minimum required separation in time to achieve decorrelation is coherence time $\mathbf{T_c}$, it is conversely proportional to the Doppler spread of the channel.

2.1.3. Practical MIMO channels

In real-world, the manner of $\mathbf{H}$ could be different from $\tilde{\mathbf{H}}$ because of the combination of inadequate antenna spacing and/or inadequate scattering which leads to spatial correlation. Also, the presence of the fixed (line-of-sight (LOS)) component in the channel results in Rician fading. In this scenario, channel elements have Rician distribution as:

$$p_Z(z) = \frac{2z(K+1)}{P_r} \exp(-K - \frac{(K+1)Z^2}{P_r}) I_0 \left(2z\sqrt{\frac{K(K+1)}{P_r}} \right) \tag{2.9}$$

where P_r is the average received power, I_0 represents the modified Bessel function of the first kind. $K \geq 0$ is the Rician K-factor of the channel and is defined as the ratio of the power in the LOS component of the channel to the power in the fading component. When $K = 0$ we have pure Rayleigh fading. At the other extreme $K = \infty$ corresponds to a non-fading channel, however, throughout this work, K is assumed to be constant. Considerable measurements have been done in the real-world to develop accurate models for MIMO channels. When LOS channel component is present in the MIMO channel model, it can be shown as a sum of a fixed and a fading component:

$$\mathbf{H} = \sqrt{\frac{K}{K+1}}\bar{\mathbf{H}} + \sqrt{\frac{1}{K+1}}\tilde{\mathbf{H}} \tag{2.10}$$

where $\bar{\mathbf{H}}$ is the fixed part, a deterministic matrix representing the Rician component of the channel, and $\tilde{\mathbf{H}}$, is the Rayleigh component and thus defined as

$$\tilde{\mathbf{H}} = \mathbf{\Sigma_r^{\frac{1}{2}} H_w \Sigma_t^{\frac{1}{2}T}} \tag{2.11}$$

MIMO channels in practice, exhibit combinations of Rician fading and spatial correlation. Furthermore, polarized antennas change the channel model and affects the performance of the MIMO signaling scheme. Knowledge of the channel at the transmitter, causes development of the signaling strategy to meet the performance requirements. The channel state information (CSI) can be complete (the precise channel realization) or partial (knowledge of the spatial correlation, K-factor, etc.).

2.2. Spatial Modulation

In general, modulation is a process of conveying message signal, inside another signal that can be physically transmitted. Frequency and amplitude modulations are the mostly used modulation schemes in telecommunication. Spatial modulation (SM), [4] is a newly introduced MIMO transmission technology for broadband wireless communication to deal with antenna synchronization and high inter-channel interference (ICI) at the receiver [28] caused by traditional MIMO systems. The basic idea behind SM is to map a block of information bits into two information conveying units: 1) A symbol that is chosen from the constellation diagram and 2) A transmit antenna number which is chosen from a set of antenna array. Using the antenna space as the information bearing unit, increases the spectral efficiency by the base-two logarithm of the number of transmit antennas. In this work only conventional-SM (C-SM) is proposed where there is only one active transmit antenna at each time instant and the ICI is avoided completely. C-SM is the specific model for generalized-SM (G-SM) where each index mapped by the antenna bits addresses a group of simultaneously activated antennas. Figure 2.3 illustrates how SM works with an example for 4 transmit antennas conveying signal over QPSK constellation. As it is shown, the input bits for transmission is assumed 1110. The first two bits (11) are assigned to a specific antenna shown by red color, where in this example it corresponds to the forth antenna, second part of the input bits (10) is mapped to the constellation diagram which is represented with yellow. For the second time instant assume 0001 is transmitted, this mapping scheme is also shown.

Table 2.1 shows a sample mapping for a system with spectral efficiency of 4 bit per channel use (bpcu) SM with 4 transmit antennas and employing QPSK constellation.

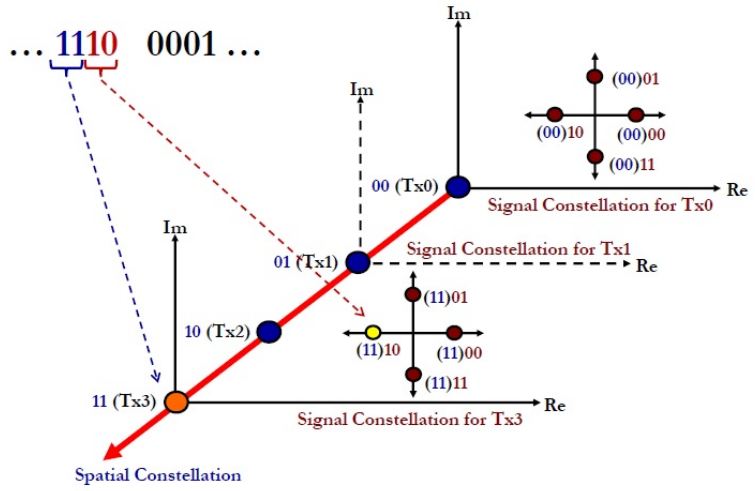

(a)

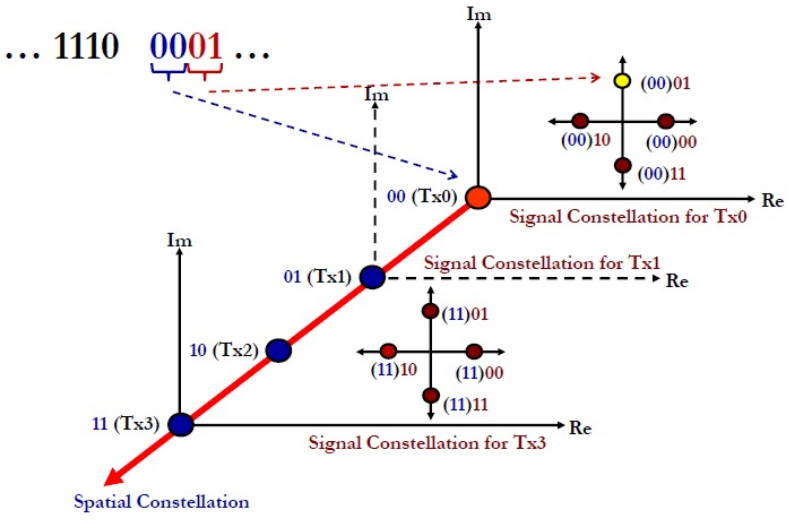

(b)

Figure 2.3. Spatial modulation technique.

Table 2.1. Mapping input bits to corresponding constellation symbols and antennas.

Incoming bits		Symbol bits	Antenna index
$\overbrace{\text{symbol bits}}$	$\overbrace{\text{antenna}}$		
0 0	0 0	00	1
0 0	0 1	00	2
0 0	1 0	00	3
0 0	1 1	00	4
0 1	0 0	01	1
0 1	0 1	01	2
0 1	1 0	01	3
0 1	1 1	01	4
1 0	0 0	10	1
1 0	0 1	10	2
1 0	1 0	10	3
1 0	1 1	10	4
1 1	0 0	11	1
1 1	0 1	11	2
1 1	1 0	11	3
1 1	1 1	11	4

3. DUAL-POLARIZED COMMUNICATION

3.1. Dual-Polarized SISO System

In multiple-input multiple-output systems, antenna spacing of at least half of the wavelength at the subscriber unit and ten wavelengths at the base station is required to achieve high multiplexing and diversity gains. Hence, antenna polarization has been recognized as an attractive strategy for MIMO systems. Polarization diversity has become an interest in recent years because it does not require any extra bandwidth or physical separation between the antennas. Advanced polarization methods such as dual-polarized antennas have been illustrated to improve the spectral efficiency of the channel in multiple antenna systems in comparison with classical MIMO systems. The two polarizations must be orthogonal for example horizontal/vertical or ± 45 slanted as shown in figure 3.1 respectively. Indeed, orthogonal polarizations offer better separation between channels, through a large decorrelation at transmit and receive sides.

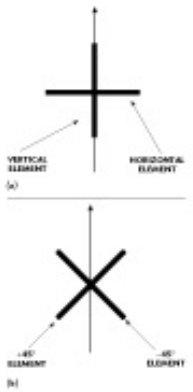

Figure 3.1. VH Polarization vs. Slanted polarization with $\pm 45^o$.

We initially analyze a single-input single-output (SISO) dual-polarized system for simplicity and to introduce coefficients which are coming from using dual-polarized antennas. In this scenario the system is equipped with a dual-polarized antenna at both sides. This can be done by either using two co-located antennas with orthogonal polarizations or a single antenna which is capable of transmitting multiple simultaneous streams via orthogonal polarizations. The polarizations at both ends do not need to be identical. For example, the transmit polarization scheme may be vertical-horizontal

(VH), while the receiver polarization is chosen to be slanted (±45 degrees). The channel matrix for the SISO system is as

$$\mathbf{H} = \begin{bmatrix} \varrho_{1_p,1_p} & \varrho_{1_p,1_{p'}} \\ \varrho_{1_{p'},1_p} & \varrho_{1_{p'},1_{p'}} \end{bmatrix} \tag{3.1}$$

where p and p' are two orthogonal polarization directions and each element of this matrix involves a fixed and a variable elements ($\bar{\varrho}$ and $\tilde{\varrho}$ respectively).

In ideal antenna cases, with a particular polarization, the received cross-polar signal amount has to be zero. However in real-world systems it is not the case and some part of the received signal comes from the polarization which is orthogonal to the desired polarization. This causes power leakages from one polarization direction to its orthogonal counterpart in the fixed and variable components of the channel. These leakage amounts are defined for fixed and variable components respectively, as $(0 < \mu_f, \mu_v \leq 1)$:

$$\begin{aligned} \mu_f &= \left|\bar{\varrho}_{1_p,1_{p'}}\right|^2 = \left|\bar{\varrho}_{1_{p'},1_p}\right|^2 \\ \mu_v &= E\left\{\left|\tilde{\varrho}_{1_p,1_{p'}}\right|^2\right\} = E\left\{\left|\tilde{\varrho}_{1_{p'},1_p}\right|^2\right\}. \end{aligned} \tag{3.2}$$

Also the co-polar terms can be defined by assuming symmetry between different polarizations as:

$$\begin{aligned} 1-\mu_f &= \left|\bar{\varrho}_{1_p,1_p}\right|^2 = \left|\bar{\varrho}_{1_{p'},1_{p'}}\right|^2 \\ 1-\mu_v &= E\left\{\left|\tilde{\varrho}_{1_p,1_p}\right|^2\right\} = E\left\{\left|\tilde{\varrho}_{1_{p'},1_{p'}}\right|^2\right\}, \end{aligned} \tag{3.3}$$

for fixed and random components respectively. The channel can de-polarized the transmitted signal, when $\mu_f = \mu_v = 0$ but for cases other than this condition, cross-polar and co-polar signals are going to be present. In this case the ratio of co-polar term to cross-polar term is characterized by XPD (cross-polar discrimination) as it is described

in [29] and [30]. The XPD factors for fixed and variable components for channel are:

$$\chi_f = \frac{1-\mu_f}{\mu_f} \quad \text{and} \quad \chi_v = \frac{1-\mu_v}{\mu_v}. \tag{3.4}$$

Larger XPD values, exhibit small cross-polar value which is the result of higher capability of the channel to de-polarize the orthogonal polarization directions. In addition smaller XPD represents more considerable cross-polar interference (XPI). In some previous works, XPD is assumed as a single term and the fixed and variable parts are not considered separately as in [14], [31] and [32]. However a line of experiments reported XPD values for different environments such as indoor [33], urban [34], suburban [33]. The overall XPD values are changing for Rician and Rayleigh fading channels, that is why we consider different μ_f and μ_v values for a generalized formulation as in [30]. The amounts of power leakages from one polarization to the other can be collected in leakage matrices for fixed and variable components of the channel as $\mathbf{\Gamma}_f$ and $\mathbf{\Gamma}_v$ respectively, defined as:

$$\mathbf{\Gamma}_f = \begin{bmatrix} \sqrt{1-\mu_f} & \sqrt{\mu_f} \\ \sqrt{\mu_f} & \sqrt{1-\mu_f} \end{bmatrix}, \tag{3.5}$$

$$\mathbf{\Gamma}_v = \begin{bmatrix} \sqrt{1-\mu_v} & \sqrt{\mu_v} \\ \sqrt{\mu_v} & \sqrt{1-\mu_v} \end{bmatrix}. \tag{3.6}$$

The XPD modeling is shown in figure 3.1 where the single polarized and dual-polarized antenna arrays are shown in it.

Furthermore, a second impact of the dual-polarized antennas is polarization correlation (XPC) between orthogonal polarization directions which comes when the scattering of the channel is poor de-polarization of signal will become a problem. This causes polarization correlation coefficients at transmitter and receiver are defined as

$$\begin{aligned} \gamma_t &= \frac{E\left\{\tilde{\varrho}_{i_p,i_p}\tilde{\varrho}^*_{i_p,i_{p'}}\right\}}{\sqrt{\mu_v\left(1-\mu_v\right)}} = \frac{E\left\{\tilde{\varrho}_{i_{p'},i_p}\tilde{\varrho}^*_{i_{p'},i_{p'}}\right\}}{\sqrt{\mu_v\left(1-\mu_v\right)}}, \\ \gamma_r &= \frac{E\left\{\tilde{\varrho}_{j_p,j_p}\tilde{\varrho}^*_{j_{p'},j_p}\right\}}{\sqrt{\mu_v\left(1-\mu_v\right)}} = \frac{E\left\{\tilde{\varrho}_{j_p,j_{p'}}\tilde{\varrho}^*_{j_{p'},j_{p'}}\right\}}{\sqrt{\mu_v\left(1-\mu_v\right)}}. \end{aligned} \tag{3.7}$$

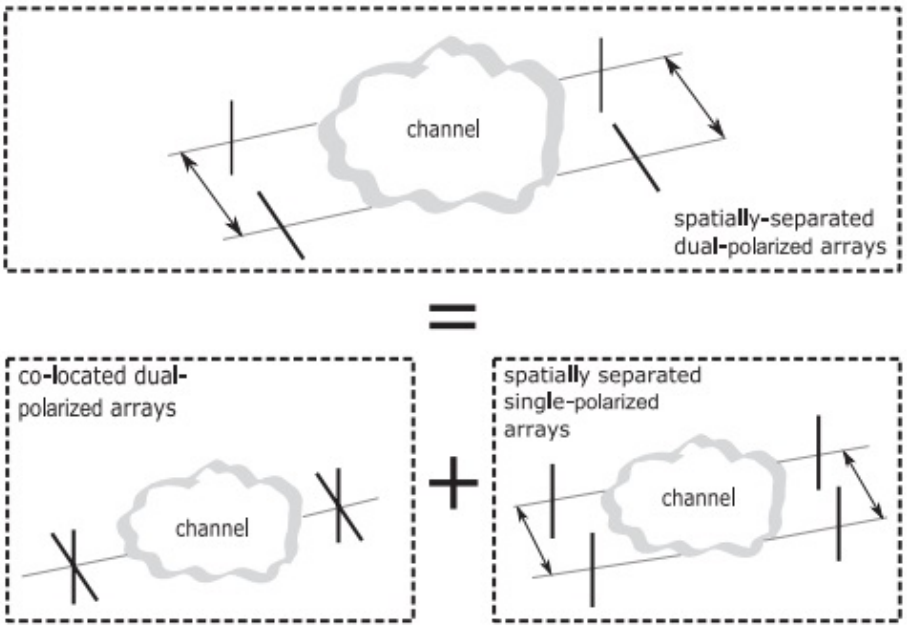

Figure 3.2. XPD modeling: separation between space and polarization.

where $0 \leq \gamma_t, \gamma_r \leq 1$ by assuming the symmetry conditions. These coefficients are assumed to be the same for all dual-polarized antennas. $\mathbf{\Pi}_{\mathrm{t}}$ and $\mathbf{\Pi}_{\mathrm{r}}$ are the polarization correlation matrices which can be modeled for SISO system as:

$$\mathbf{\Pi}_{\mathrm{t}} = \begin{bmatrix} 1 & \gamma_t \\ \gamma_t^* & 1 \end{bmatrix}, \qquad \mathbf{\Pi}_{\mathrm{r}} = \begin{bmatrix} 1 & \gamma_r \\ \gamma_r^* & 1 \end{bmatrix}. \tag{3.8}$$

Consequently, by considering transmit and receive polarization coefficients, XPD and XPC, the Rayleigh channel model for SISO system becomes as:

$$\mathbf{H} = \mathbf{\Gamma}_v \odot \left(\mathbf{\Pi}_{\mathrm{r}}^{\frac{1}{2}} \mathbf{H}_w \mathbf{\Pi}_{\mathrm{t}}^{\frac{1}{2}T} \right) \tag{3.9}$$

where $\mathbf{H}_w$ is a 2×2 channel matrix, with independent circularly symmetric zero mean complex Gaussian elements. The operator $\odot$ denotes the element by element Hadamard multiplication.

Additionally, the Rician channel becomes as:

$$\mathbf{H} = \sqrt{\frac{K}{K+1}}\mathbf{\Gamma}_f \odot \overline{\overline{\mathbf{H}}} + \sqrt{\frac{1}{K+1}}\mathbf{\Gamma}_v \odot \left(\mathbf{\Pi}_{\mathrm{r}}^{\frac{1}{2}}\mathbf{H}_w\mathbf{\Pi}_{\mathrm{t}}^{\frac{1}{2}T}\right) \tag{3.10}$$

$\overline{\overline{\mathbf{H}}}$ is a 2×2 deterministic matrix for line-of-sight coefficients where it is chosen as an all one matrix as also done in [30], [35] and K is the Rician factor. Notice that in this work, we assume a vertical and horizontal (VH) model for polarizations of the all transmit and receive antennas. But there are alternative polarization schemes as in [30] and [36] for channel model which might be done by using unitary rotation transformations to $\mathbf{H}$ such as:

$$\mathbf{H}_{rot} = \mathbf{R}_r\mathbf{H}\mathbf{R}_t \tag{3.11}$$

where $\mathbf{R}_t$ and $\mathbf{R}_r$ are the transmit and receive rotation matrices respectively as:

$$\mathbf{R}_{\mathrm{t}} = \begin{bmatrix} \cos\theta_t & -\sin\theta_t \\ \sin\theta_t & \cos\theta_t \end{bmatrix}, \qquad \mathbf{R}_{\mathrm{r}} = \begin{bmatrix} \cos\theta_r & -\sin\theta_r \\ \sin\theta_r & \cos\theta_r \end{bmatrix}. \tag{3.12}$$

Here θ_t and θ_r denote the angles of rotations related to vertical direction at the transmitter and the receiver in order. $\theta_t = \theta_r = 0^o$ corresponds to vertical and horizontal (VH) polarizations, also $\theta_t \neq \theta_r$ corresponds to polarization mismatch.

3.2. MIMO Dual-Polarized Systems

In this section, we extend our analysis to spatially separated multiple dual-polarized antennas which adds spatial correlation coefficient to the system. Assume a $M \times N$ MIMO channel with dual-polarized antennas. Channel matrix can be defined

as a $2N \times 2M$ dimensional matrix as:

$$\mathbf{H} = \begin{bmatrix} \varrho_{1_p,1_p} & \varrho_{1_p,1_{p'}} & \varrho_{1_p,2_p} & \cdots & \varrho_{1_p,M_{p'}} \\ \varrho_{1_{p'},1_p} & \varrho_{1_{p'},1_{p'}} & \varrho_{1_{p'}h,2_p} & \cdots & \varrho_{1_{p'},M_{p'}} \\ \varrho_{2_p,1_p} & \varrho_{2_p,1_{p'}} & \varrho_{2_p,2_p} & \cdots & \varrho_{2_p,M_{p'}} \\ \varrho_{2_{p'},1_p} & \varrho_{2_{p'},1_{p'}} & \varrho_{2_{p'},2_p} & \cdots & \varrho_{2_{p'},M_{p'}} \\ \vdots & \vdots & \vdots & \vdots & \vdots \\ \varrho_{N_p,1_p} & \varrho_{N_p,1_{p'}} & \varrho_{N_p,2_p} & \cdots & \varrho_{N_p,M_{p'}} \\ \varrho_{N_{p'},1_p} & \varrho_{N_{p'},1_{p'}} & \varrho_{N_{p'},2_p} & \cdots & \varrho_{N_{p'},M_{p'}} \end{bmatrix} \tag{3.13}$$

where ϱ_{i_u,j_v} represents the observed channel coefficients between the polarization direction u of the i-th receive antenna and the polarization direction of v of the j-th transmit antenna, for $i = 1 \ldots N$, $j = 1 \ldots M$ and $u, v \in \{p, p'\}$. By this assumption, elements with $u = v$ and $u \neq v$ represent the co-polar and cross-polar channel coefficients, in order. Facilitation of the model, might be done combining the polarization direction and antenna indices to one channel index, so $\mathbf{H}$ can be expressed as a simple one-to-one mapping presented below as:

$$\mathbf{H} = \begin{bmatrix} h_{1,1} & h_{1,2} & \cdots & h_{1,(2M)} \\ h_{2,1} & h_{2,2} & \cdots & h_{2,(2M)} \\ h_{3,1} & h_{3,2} & \cdots & h_{3,(2M)} \\ h_{4,1} & h_{4,2} & \cdots & h_{4,(2M)} \\ \vdots & \vdots & \vdots & \vdots \\ h_{(2N-1),1} & h_{(2N-1),2} & \cdots & h_{(2N-1),(2M)} \\ h_{(2N),1} & h_{(2N),2} & \cdots & h_{(2N),(2M)} \end{bmatrix} \tag{3.14}$$

This mapping is going to be used in this work for the sake of simplicity. A slow fading MIMO channel is assumed which includes a fixed (LOS) and a variable parts. also identical scattering environment is assumed for all antennas at both sides. The channel model is as it is shown in (2.10), where in addition to polarization correlations, spatial correlation matrices, $\mathbf{\Sigma_t}$ and $\mathbf{\Sigma_r}$, are present due to the multiple antenna utilization.

Considering the aforementioned conditions, $\bar{\mathbf{H}}$ in (2.10) can be written as

$$\bar{\mathbf{H}} = (\mathbf{1}_{N\times M} \otimes \mathbf{\Gamma}_f) \odot \overline{\overline{\mathbf{H}}} \tag{3.15}$$

where $\overline{\overline{\mathbf{H}}}$ is the fixed part of the channel, a 2×2 deterministic matrix as defined before, such that $\left[\overline{\overline{\mathbf{H}}}\right]_{p,q} = \overline{h}_{p,q}$, for $p = 1,\ldots,2N$ and $q = 1,\ldots,2M$. The elements of $\overline{\overline{\mathbf{H}}}$ are assumed to be all one for simplicity. $\mathbf{1}_{N\times M}$ is an $N \times M$ matrix with all one elements and $\otimes$ stands for the Kronecker product.

The variable component of the channel matrix, $\tilde{\mathbf{H}}$ consists of possibly correlated complex Gaussian variables, given $\left[\tilde{\mathbf{H}}\right]_{p,q} = \tilde{h}_{p,q}$, for channel coefficients pairs $(\tilde{h}_{p,q}, \tilde{h}_{\hat{p},\hat{q}})$ with $p,\hat{p} = 1,\ldots,2N$ and $q,\hat{q} = 1,\ldots,2M$. We suppose that the real and imaginary parts have equal auto-correlations and real and imaginary parts are not correlated:

$$\begin{aligned} E\left[\tilde{h}^R_{p,q}\tilde{h}^R_{\hat{p},\hat{q}}\right] &= E\left[\tilde{h}^I_{p,q}\tilde{h}^I_{\hat{p},\hat{q}}\right], \\ E\left[\tilde{h}^R_{p,q}\tilde{h}^I_{\hat{p},\hat{q}}\right] &= E\left[\tilde{h}^I_{p,q}\tilde{h}^R_{\hat{p},\hat{q}}\right] = 0 \end{aligned} \tag{3.16}$$

Furthermore, with these conditions, the channel matrix which is correlated would be defined by the Kronecker correlation model, so $\tilde{\mathbf{H}}$ can be shown by:

$$\tilde{\mathbf{H}} = \dot{\mathbf{H}} \otimes \ddot{\mathbf{H}} \tag{3.17}$$

where $\dot{\mathbf{H}}$ is a matrix with possibly correlated elements defined as $\left[\dot{\mathbf{H}}_{p,q}\right] = re^{j\theta}$ and $\ddot{\mathbf{H}}$ is a matrix defined as $\left[\ddot{\mathbf{H}}_{p,q}\right] = e^{j\phi}$, which models the rotation of the polarization and correlated phase between four channels created by 1×1 dual-polarized antennas. We can define each term of $\dot{\mathbf{H}}$ and $\ddot{\mathbf{H}}$ by using [29] and [31] as:

$$\dot{\mathbf{H}} = \mathbf{\Sigma}_{\mathbf{r}}^{\frac{\mathbf{1}}{\mathbf{2}}} \dot{\mathbf{H}}_{\mathbf{w}} \mathbf{\Sigma}_{\mathbf{t}}^{\frac{\mathbf{1}}{\mathbf{2}}\mathbf{T}} \tag{3.18}$$

Where $\dot{\mathbf{H}}_w$ is a $N \times M$ Rayleigh fading channel matrix, with variables of i.i.d. complex Gaussian distribution, i.e.,$\sim \mathcal{CN}(0,1)$. So the variable part of the channel becomes as:

$$\tilde{\mathbf{H}} = (\mathbf{1}_{N\times M} \otimes \mathbf{\Gamma}_v) \odot \left(\Phi_{\mathrm{r}}{}^{\frac{1}{2}} \mathbf{H}_w \Phi_{\mathrm{t}}{}^{\frac{1}{2}}\right) \tag{3.19}$$

where $\Phi_{\mathbf{r}} = \mathbf{\Sigma}_{\mathbf{r}} \otimes \mathbf{\Pi}_{\mathbf{r}}$, $\Phi_{\mathbf{t}} = \mathbf{\Sigma}_{\mathbf{t}} \otimes \mathbf{\Pi}_{\mathbf{t}}$. $\Phi_{\mathbf{t}}$ and $\Phi_{\mathbf{r}}$ are $2M \times 2M$ and $2N \times 2N$ real valued and Hermitian symmetric transmit and receive correlation matrices, respectively. After employing Kronecker product, $\mathbf{H}_w$ becomes independent Rayleigh fading channel matrix, with elements described as i.i.d complex Gaussian random variables.$[\mathbf{H}_w]_{p,q} = h_{wp,q} \sim \mathcal{CN}(0,1)$ for $p = 1 \ldots 2N$ and $q = 1 \ldots 2M$. Accordingly, the general formulation for channel matrix with dimension of $M \times N$ using dual-polarized antennas may be shown as:

$$\begin{aligned} \mathbf{H} &= \sqrt{\frac{K}{1+K}} (\mathbf{1}_{N\times M} \otimes \mathbf{\Gamma}_f) \odot \overline{\overline{\mathbf{H}}} \\ &+ \sqrt{\frac{1}{1+K}} (\mathbf{1}_{N\times M} \otimes \mathbf{\Gamma}_v) \odot \left(\Phi_{\mathrm{r}}{}^{\frac{1}{2}} \mathbf{H}_w \Phi_{\mathrm{t}}{}^{\frac{1}{2}}\right). \end{aligned} \tag{3.20}$$

The equivalent MIMO system using uni-polarized antennas is a $2N \times 2M$ matrix defined as:

$$\mathbf{H}' = \sqrt{\frac{K}{K+1}} \bar{\mathbf{H}}' + \sqrt{\frac{1}{K+1}} \tilde{\mathbf{H}}' \tag{3.21}$$

where $\bar{\mathbf{H}}'$ is a $2N \times 2M$ deterministic matrix, $\tilde{\mathbf{H}}' = \Phi_{\mathbf{r}}'^{\frac{1}{2}} \tilde{\mathbf{H}}'_{\mathbf{w}} \Phi_{\mathbf{t}}'^{\frac{1}{2}\mathbf{T}}$ with $\Phi'_{\mathbf{r}} = \mathbf{\Sigma}'_{\mathbf{r}}$ and $\Phi'_{\mathbf{t}} = \mathbf{\Sigma}'_{\mathbf{t}}$ which are $2N \times 2N$ and $2M \times 2M$ dimensional matrices of spatial correlation for receiver and transmitter sides respectively. $\tilde{\mathbf{H}}'_w$ is a $2N \times 2M$ independent Rayleigh fading channel matrix, with elements following $\left[\tilde{\mathbf{H}}'_w\right]_{p,q} = \tilde{h'}_{wp,q} \sim \mathcal{CN}(0,1)$ for $p = 1, \ldots, 2N$ and $q = 1, \ldots, 2M$.

3.3. Dual-Polarized Spatial Modulation System

Here a system with M transmit and N receive dual-polarized antennas as in [17], is considered. $M \times N$ dual-polarized system is equivalent to $2M \times 2N$ MIMO system. The transmit antenna number is supposed to be an integer power of 2, for simplicity, $M = 2^m$, also we consider an *L-ary* constellation, with ℓ bits assigning to constellation $\mathcal{X} = \{X_1, \dots X_k, \dots X_L\}$ which consists of L symbols so $\ell = \log_2 L$. Transmitted bits are split into $m + \ell + 1$ bits, where m bits are used to select the active antenna, ℓ bits to choose from constellation symbols and one bit is used to select the polarization direction. In this system the spectral efficiency is $R = m + \ell + 1 = \log_2(2ML)$ bits per channel use (bpcu). Table (3.1) shows the mapping strategy for dual-polarized SM system with spectral efficiency of $R = 4$ bpcu, with two transmit antennas and using QPSK modulation and polarization directions orthogonal to each other shown by p and p'.

The transmitted signal vector $\mathbf{x}$ is a $2M \times 1$ vector such as $\mathbf{x} = \Big[\mathbf{x}_1, \dots \mathbf{x}_\ell, \dots \mathbf{x}_{2M}\Big]^{\mathbf{T}}$, where all entries of $\mathbf{x}$ are zero except one entry. The location of the nonzero element of $\mathbf{x}$, shows the chosen activated antenna and its active polarization direction, and its value shows the symbol chosen from the modulation alphabet, respectively. Constraint power of unity, i.e. $E_{\mathbf{x}}[\mathbf{x}^H\mathbf{x} = 1]$ is assumed. The signal which is modulated is transmitted through the channel which is modeled with the matrix in (3.14), and is received by N dual-polarized antennas. Consequently, we can model the received signal by:

$$\mathbf{y} = \mathbf{H}\mathbf{x} + \mathbf{n} \tag{3.22}$$

where $\mathbf{y}$ and $\mathbf{n}$ are $2N \times 1$ received signal and noise vectors respectively, $\mathbf{H}$ is $2N \times 2M$ channel matrix as shown in (3.14), and $\mathbf{x}$ is a $2M \times 1$ transmitted signal vector. $\mathbf{n}$ has independent and identically distributed (i.i.d.) complex Gaussian random variables with zero mean and variance N_0, i.e., $\mathbf{n}_k \sim \mathcal{CN}(0, N_0)$ for $k = 1, \dots, 2N$, thus the SNR is described as $\eta = \frac{E_s}{N_0} = \frac{1}{N_0}$. Suppose that the v-th component X_v for $v = 1, \dots, L$, from the constellation alphabet, is transmitted. Because only one entry of $\mathbf{x}$ is non-zero,

Table 3.1. Mapping information bits into antenna, polarization direction and constellation symbol.

Incoming bits				Symbol bits	Antenna	Polarization	X_s
symbol bits		*antenna*	*polarization*				
0	0	0	0	00	1	p	1
0	0	0	1	00	1	p'	1
0	0	1	0	00	2	p	1
0	0	1	1	00	2	p'	1
0	1	0	0	01	1	p	j
0	1	0	1	01	1	p'	j
0	1	1	0	01	2	p	j
0	1	1	1	01	2	p'	j
1	0	0	0	10	1	p	-1
1	0	0	1	10	1	p'	-1
1	0	1	0	10	2	p	-1
1	0	1	1	10	2	p'	-1
1	1	0	0	11	1	p	-j
1	1	0	1	11	1	p'	-j
1	1	1	0	11	2	p	-j
1	1	1	1	11	2	p'	-j

equation (3.22) can be rewritten as

$$\mathbf{y} = \mathbf{h}_u X_v + \mathbf{n} \tag{3.23}$$

$\mathbf{h}_u$ stands for the u-th column of $\mathbf{H}$ where u corresponds to a transmit antenna which is activated and its polarization direction pair (u', j) for $u' = 1, 2, \cdots, M$ and $j = p, p'$.

4. PRECODED DUAL-POLARIZED SPATIAL MODULATION

4.1. System Model

A precoding approach is presented in this part of the work for DP-SM MIMO system, to make the system more resistant to corruptions caused by channel, for example LOS component influences and also spatial correlations among transmit antennas. This technique which is based on the rotation of the phase and/or amplitude scaling of the transmitted symbols in accordance with the active transmit antenna, can be implemented while keeping the average power budget and without any explicit knowledge of the channel state information (CSI) at the transmitter. This means multiplying the transmitted symbol vector $\mathbf{x}$ as defined in the previous chapter with a matrix of precoding which is diagonal as

$$\begin{aligned} \mathbf{\Psi} &= \mathbf{Diag}\begin{bmatrix}\psi_1 & \psi_2 & \dots & \psi_{2M}\end{bmatrix} \\ &= \mathbf{Diag}\begin{bmatrix}a_1 e^{j\theta_1} & a_2 e^{j\theta_2} & \dots & a_{2M} e^{j\theta_{2M}}\end{bmatrix}, \end{aligned} \tag{4.1}$$

where for non-modified average power budget, the coefficients in precoder matrix must fulfill the shown situation:

$$\frac{1}{2M}\sum_{\ell=1}^{2M}|\psi|_\ell^2 = \frac{1}{2M}\sum_{\ell=1}^{2M}a_\ell^2 = 1. \tag{4.2}$$

Our precoder design is based on determination of the $2M-1$ optimum values of phase rotation, because the assumption is that there is no rotation for symbols transmitted from the first polarization of the first antenna, and $2M$ optimum values for amplitude coefficients. Furthermore, simpler applications are available such as deploying just rotations for phases and supposing $a_l = 1$ for all $l = 1, \dots, 2M$. This scheme decreases the search space for the optimization of the precoding matrix in addition to the prevention of power fluctuations which is the result of the avoidance of amplitude scaling. An other model could be the application of just scale of the amplitude (or

power control) by deleting the rotations for phase values. In our work, we do the precoding operation by only constellation rotations based on the active polarization of the active antenna, and there is no amplitude scaling assumed to make the optimization and implementation more easy. The precoding matrix can be rewritten as:

$$\begin{aligned} \mathbf{\Psi} &= \mathbf{Diag}\begin{bmatrix}\psi_1 & \psi_2 & \dots & \psi_{2M}\end{bmatrix} \\ &= \mathbf{Diag}\begin{bmatrix}e^{j\theta_1} & e^{j\theta_2} & \dots & e^{j\theta_{2M}}\end{bmatrix}. \end{aligned} \tag{4.3}$$

The corresponding received signal can be written as

$$\mathbf{y} = \mathbf{H}\mathbf{\Psi}\mathbf{x} + \mathbf{n} \tag{4.4}$$

$\mathbf{n}$ and $\mathbf{y}$ are the $2N \times 1$ dimensional channel noise and received signal vectors, respectively. $\mathbf{H}$ is a channel matrix with $2N \times 2M$ dimension as defined in (3.14) and $\mathbf{x}$ is the transmitted signal vector as defined before. If we suppose that the v-th component of the constellation, X_v for $v = 1, \dots, L$, is transmitted as before, equation (4.4) can be rewritten as:

$$\mathbf{y} = \mathbf{h}_u X_v e^{j\theta_u} + \mathbf{n} \tag{4.5}$$

where $\mathbf{h}_u$ identifies the u-th column of $\mathbf{H}$ with u corresponding to a single active transmit antenna and polarization direction pair (u', j) for $u' = 1, 2, \cdots, M$ and $j = p, p'$. As referred in previous chapters, a slow fading channel is assumed which is the summation of a fixed (or average, LOS) and a variable (or random, NLOS) parts. The channel model was shown in (3.20).

Given the signal model in (4.5) and model for MIMO system in (3.20), the receiver uses maximum likelihood (ML) detection rule to detect the single transmit antenna and polarization direction and the chosen symbol from the constellation. Because we can combine the transmit antenna and polarization directions into a single channel index as shown in (3.14), receiver estimates the most probable channel and symbol index pair

$(u, v)_{ML}$ given as

$$(u_{\mathbf{ML}}, v_{\mathbf{ML}}) = \arg\min_{u,v} D(\mathbf{y}|\mathbf{h}_u, X_v, \mathbf{\Psi}) \tag{4.6}$$

where $D(\mathbf{y}|\mathbf{h}_u, X_v, \mathbf{\Psi}) = \|\mathbf{y} - \mathbf{h}_u X_v e^{j\theta_u}\|^2$ is the distance metric, which the receiver tries to find the indices which make this metric minimum. Once the most likely channel index is found it is easy to detect the indices of the most likely antenna and polarization direction by the use of mapping plan in (3.14).

4.2. Performance Analysis and Precoder Design

4.2.1. Perfect Channel Estimation

The main mission for precoding matrix $\mathbf{\Psi}$ designation is to specify the optimal values of rotation angles θ_ℓ's for $\ell = 2, 3, ..., 2M$. A time-varying fading channel is considered where there is no information about the channel available at the transmitter, so our design is based on the minimization of the average bit-error probability, which is done in high SNR values. In this section, a pairwise error probability (PEP) is calculated to find the average pairwise error probability (APEP) of the precoded DP-SM system. Once the APEP is calculated, it is easy to approximate the average bit error probability (ABEP) by the well-known upper bound as in [37]:

$$\bar{P}_b \leq \frac{1}{2ML} \sum_{u=1}^{2M} \sum_{\hat{u}=1}^{2M} \sum_{v=1}^{L} \sum_{\hat{v}=1}^{L} \frac{N(u, \hat{u}, v, \hat{v})}{\log_2(2ML)} \bar{P}_s(u, \hat{u}, \psi_u, \psi_{\hat{u}}, v, \hat{v}) \tag{4.7}$$

where $N(u, \hat{u}, v, \hat{v})$ identifies the number of bits in error between the respective channel and symbol pairs, $(\mathbf{h}_u, X_v)$ and $(\mathbf{h}_{\hat{u}}, X_{\hat{v}})$, and $\bar{P}_s(u, \hat{u}, \psi_u, \psi_{\hat{u}}, v, \hat{v})$ is the identical average pairwise symbol error probability (APEP). $\log_2(2ML) = m + \ell + 1$ identifies the entire number of bits utilized for detecting the direction of the polarization, active antenna and the symbol. The necessary part of computing the ABEP upper bound is to calculate the pairwise error probabilities (PEP's) and computing the expected values as shown in the following. PEP identifies the probability of error for detecting the channel and symbol pair $(\mathbf{h}_{\hat{u}}, X_{\hat{v}})$ instead of the exact pair $(\mathbf{h}_u, X_v)$ as the following

equation:

$$P_s(u, \hat{u}, \psi_u, \psi_{\hat{u}}, v, \hat{v}) = Q\left(\sqrt{\frac{\| \mathbf{z} \|^2}{2}}\right) \tag{4.8}$$

where $\mathbf{z}$ is a $2N \times 1$ vector described in [5]

$$\mathbf{z} = \frac{1}{\sqrt{N_0}}(\mathbf{h}_u \psi_u X_v - \mathbf{h}_{\hat{u}} \psi_{\hat{u}} X_{\hat{v}}), \tag{4.9}$$

It can be shown that $\mathbf{z}$ is a Gaussian vector with complex elements and joint PDF of:

$$f_{\mathbf{Z}}(\mathbf{z}|\mathbf{h}_u, \mathbf{h}_{\hat{u}}, \psi_u, \psi_{\hat{u}}, X_v, X_{\hat{v}}) = \frac{e^{-(\mathbf{z}-\mathbf{m_z})^H \mathbf{\Lambda_z}^{-1}(\mathbf{z}-\mathbf{m_z})}}{\pi^{2N}|\mathbf{\Lambda_z}|} \tag{4.10}$$

where the mean and covariance of $\mathbf{z}$ defined as $\mathbf{m_z}$ and $\mathbf{\Lambda_z}$, are computed as

$$\mathbf{m_z} = \mathrm{E}[\mathbf{z}] = \sqrt{\frac{K}{N_0(K+1)}}(\overline{\mathbf{h}}_u \psi_u X_v - \overline{\mathbf{h}}_{\hat{u}} \psi_{\hat{u}} X_{\hat{v}}) \tag{4.11}$$

$$\begin{aligned} \mathbf{\Lambda_z} &= \mathrm{E}\left[(\mathbf{z}-\mathbf{m_z})(\mathbf{z}-\mathbf{m_z})^{\mathbf{H}}\right] \\ &= \frac{\phi^t_{u,u}|X_v|^2 + \phi^t_{\hat{u},\hat{u}}|X_{\hat{v}}|^2 - 2\,\mathrm{Re}\{\phi_{u,\hat{u}} e^{j(\theta_u - \theta_{\hat{u}})} X_v X^*_{\hat{v}}\}}{N_0(K+1)} \mathbf{\Phi}_r \end{aligned} \tag{4.12}$$

with $\phi^{\mathbf{t}}_{\mathbf{i,j}}$ identifying the (i,j)-th entry of the correlation matrix at the transmitter side Φ_t which was defined before and denotes the correlation contributions of the transmission parameters. Then by the use of Q-function formulation in addition to moment generating function (MGF), the APEP in (4.7) could be calculated by

$$\begin{aligned} \bar{P}_s(u, \hat{u}, \psi_u, \psi_{\hat{u}}, v, \hat{v}) &= \int_{\mathbf{z}} Q\left(\sqrt{\frac{\| \mathbf{z} \|^2}{2}}\right) f_{\mathbf{Z}}(\mathbf{z}|\mathbf{h}_u, \mathbf{h}_{\hat{u}}, \psi_u, \psi_{\hat{u}}, X_v X_{\hat{v}}) d\mathbf{Z} \\ &= \frac{1}{\pi}\int_0^{\frac{\pi}{2}} \frac{\exp\left(-\mathbf{m}^{\dagger}_{\mathbf{z}}[\mathbf{\Lambda_z} + 4\sin^2\theta \mathbf{I}]^{-1}\mathbf{m_z}\right)}{\left|\frac{\mathbf{\Lambda_z}}{4\sin^2\theta} + \mathbf{I}\right|} d\theta \end{aligned} \tag{4.13}$$

Where $\mathbf{m_z}$ and $\mathbf{\Lambda_z}$ are as defined in (4.11) and (4.12). For the case of Rayleigh channels with $K = 0$, the exponential term will be omitted in (4.13) and the calculation of APEP is possible. However, when the channel has LOS component where $K \neq 0$, the equation in (4.13) does not simplify any further, but an upper bound can be derived for both channel scenarios by simply setting $\sin\theta = 1$ in (4.13) as

$$\begin{aligned} \bar{P}_s(u,\hat{u},\psi_u,\psi_{\hat{u}},v,\hat{v}) &= \frac{1}{\pi}\int_0^{\frac{\pi}{2}} \frac{\exp\left(-\mathbf{m}_\mathbf{z}^\dagger[\mathbf{\Lambda_z}+4\sin^2\theta\mathbf{I}]^{-1}\mathbf{m_z}\right)}{\left|\frac{\mathbf{\Lambda_z}}{4\sin^2\theta}+\mathbf{I}\right|}d\theta \\ &\leq \frac{1}{2}\frac{\exp\left(-\mathbf{m}_\mathbf{z}^\dagger[\mathbf{\Lambda_z}+4\mathbf{I}]^{-1}\mathbf{m_z}\right)}{\left|\frac{\mathbf{\Lambda_z}}{4}+\mathbf{I}\right|}. \end{aligned} \tag{4.14}$$

Notice that after the computation of APEP's between all channels and symbol pairs, they are utilized to compute the average bit error probability upper bound in (4.7). We can not achieve a closed-form resolution for the optimal set of coefficients in the precoding matrix $\hat{\mathbf{\Psi}}$ which minimizing the upper bound, but we may find this optimum matrix by numerical search algorithms at high SNR values.

Another way to calculate the APEP upper bound is to use the alternate and a noted formulation in which the received signal is rewritten as

$$\mathbf{y} = (\mathbf{x}^T\mathbf{\Psi}\otimes\mathbf{I}_N)vec(\mathbf{H}) + \mathbf{n} \tag{4.15}$$

with

$$vec(\mathbf{H}) = \sqrt{\frac{K}{1+K}}vec(\bar{\mathbf{H}}) + \sqrt{\frac{1}{1+K}}\mathbf{\Delta}^{\frac{1}{2}}vec(\tilde{\mathbf{H}}_w) \tag{4.16}$$

where $\mathbf{\Delta}^{\frac{1}{2}} = vec\left(\mathbf{1}_{N\times M}\otimes\mathbf{\Gamma}_v\right)\circ\Phi^{\frac{1}{2}}$, $\circ$ is row-wise product and $\Phi = \Phi_t^T\otimes\Phi_r$.

The vector $\mathbf{z}$ that appeared in (4.9), becomes

$$\mathbf{z} = \sqrt{\frac{K}{N_0(1+K)}}\mathbf{\Upsilon}(u,\hat{u},v,\hat{v})vec(\bar{\mathbf{H}}) + \sqrt{\frac{1}{N_0(1+K)}}\mathbf{\Upsilon}(u,\hat{u},v,\hat{v})\mathbf{\Delta}^{\frac{1}{2}}vec(\tilde{\mathbf{H}}_w) \tag{4.17}$$

where $\boldsymbol{\Upsilon}(u,\hat{u},v,\hat{v}) = (\mathbf{x}_{u,v}^T\boldsymbol{\Psi}_{u,u} - \mathbf{x}_{\hat{u},\hat{v}}^T\boldsymbol{\Psi}_{\hat{u},\hat{u}}) \otimes \mathbf{I}_N$. Then, given $\mathbf{z}$ as in (4.17), the mean vector and covariance matrix are computed by

$$\begin{aligned} \mathbf{m}_z &= \sqrt{\frac{K}{N_0(1+K)}}\boldsymbol{\Upsilon}(u,\hat{u},v,\hat{v})vec(\bar{\mathbf{H}}) \\ \boldsymbol{\Lambda}_z &= \frac{\boldsymbol{\Upsilon}(u,\hat{u},v,\hat{v})\boldsymbol{\Delta}\boldsymbol{\Upsilon}^\dagger(u,\hat{u},v,\hat{v})}{N_0(1+K)}. \end{aligned} \tag{4.18}$$

By using the shown equations, the approximate upper bound in (4.14) changes into:

$$\begin{aligned} \bar{P}_s(u,\hat{u},\psi_u,\psi_{\hat{u}},v,\hat{v}) \quad &\leqslant \tfrac{1}{2}\tfrac{1}{|\mathbf{A}|}\exp(\tfrac{-K}{4N_0(1+K)} \times \\ & tr\big[\,(\boldsymbol{\Upsilon}(u,\hat{u},v,\hat{v}))\,vec(\bar{\mathbf{H}})vec(\bar{\mathbf{H}})^\dagger\boldsymbol{\Upsilon}^\dagger(u,\hat{u},v,\hat{v})\mathbf{A}^{-1}\big]) \end{aligned} \tag{4.19}$$

where $tr[\cdot]$ is defined as the matrix trace operator and

$$\mathbf{A} = \mathbf{I} + \frac{\boldsymbol{\Upsilon}(u,\hat{u},v,\hat{v})\boldsymbol{\Delta}\boldsymbol{\Upsilon}^\dagger(u,\hat{u},v,\hat{v})}{4N_0(1+K)}. \tag{4.20}$$

We can show that the equations (4.19) and (4.14) are equal.

4.2.2. Erroneous Channel Estimation

In the previous section, we have considered that the receiver estimates channel perfectly and the precoded dual-polarized SM detection was done without channel estimation errors. Nevertheless, in real-world, the receiver might not estimate the channel perfectly and it results into an estimation error. In this part of the work the unfavorable influences of the erroneous estimation of channel on the performance of the system is considered as it has been shown in [38] completely. The pairwise error probability for the DP-SM system is computed when channel estimation errors are present and the upper bound for the ABEP is approximated for M-PSK and M-QAM modulations. We represent that the upper bound evaluation is in tight agreement especially for high SNR values with the simulation results, and DP-SM is quite robust to channel

estimation errors. A conventional approach when the channel experiences uncorrelated fading, is modeling the error as an independent and zero mean additive white Gaussian distribution on each channel fading coefficient as in [6], [38], [39]. Because the system experiences spatial and polarization correlations due to insufficient spacing and dual polarized antennas respectively, at the transmitter and/or receiver sides, we can model the estimation errors in a way that they are influenced by the correlation impacts to a specific amount. For this reason, $\mathbf{G}$ is defined as the general model for DP-SM MIMO channel which includes correlated estimation errors such as

$$\mathbf{G} = \sqrt{\frac{K}{K+1}}\bar{\mathbf{H}} + \sqrt{\frac{1}{K+1}}\left(\mathbf{1}_{N\times M} \otimes \mathbf{\Gamma}_v\right) \odot \left(\Phi_r^{\frac{1}{2}} \mathbf{H}_w \Phi_t^{\frac{1}{2}T} + \Xi_r^{\frac{1}{2}} \mho \Xi_t^{\frac{1}{2}T}\right) \tag{4.21}$$

where $\mho$ is a zero-mean additive Gaussian estimation error matrix. The elements of the error matrix $\mho$, $\delta_{i,j}$ are defined as independent and identically distributed complex Gaussian variables with zero mean and variance of σ_e^2, i.e., $\delta_{i,j} \sim \mathcal{C}N(0, \sigma_e^2)$. Two different scenarios can be considered for erroneous channel estimation as 1) Fixed σ_e^2, when the variance of the error matrix is assumed as a fix number for changing SNR values in order to show the pure effect of the imperfect channel estimation on the error performance. 2) Variable σ_e^2, when the variance of the estimation error is dependent on SNR. In this work the fixed $\sigma_e^2 = 0.01$ is assumed. Furthermore $\delta_{i,j}$'s are independent of the corresponding channel coefficients $\tilde{h}_{i,j}$.

We assume the Kronecker model to describe the spatial correlation effects on estimation errors, however the correlation matrices does not require to be equal with correlation effects on the channel coefficients. By considering it, we can separate the correlation effects at the transmitter and the receiver sides for the estimation errors as Ξ_t and Ξ_r, in order. The proposed approach enables the derivation of a general equation for many different cases of spatial correlation and error cases. The outcomes for other scenarios such as fully uncorrelated errors, errors having the same correlation effects as the channel coefficients or errors with transmit or receive only correlations may be got from the general formulation by properly choosing the respective correlation matrices. By using channel model in (4.21), the maximum likelihood detection rule

which tries to minimize the distance metric $D(u,v)$ becomes as

$$D(u,v) = (\mathbf{y} - \mathbf{m}_{u,v})^H \, \mathbf{\Lambda}_{u,v}^{-1} \, (\mathbf{y} - \mathbf{m}_{u,v}) + \log |\mathbf{\Lambda}_{u,v}|. \tag{4.22}$$

Here, $\mathbf{m}_{u,v}$ and $\mathbf{\Lambda}_{u,v}$ are the mean vector and the covariance matrix of the received signal when the channel estimation is erroneous, respectively, which are calculated as,

$$\mathbf{m}_{u,v} = \mathrm{E}\left[\mathbf{y} \mid \mathbf{g}_u, \psi_u, X_v\right] = \sqrt{\frac{K}{(K+1)}} \, (\mathbf{I} - \mathbf{\Omega}_r) \, \bar{\mathbf{h}}_u \psi_u X_v + \mathbf{\Omega}_r \mathbf{g}_u \psi_{\hat{u}} X_v \tag{4.23}$$

$$\mathbf{\Lambda}_{u,v} = \mathrm{E}\left[(\mathbf{y} - \mathbf{m}_{u,v}) \, (\mathbf{y} - \mathbf{m}_{u,v})^H \mid \mathbf{g}_u, \psi_u, X_v\right] = \frac{1}{\eta}\mathbf{I} + \frac{|X_v|^2}{K+1} \, (\wp_{\mathbf{u},\mathbf{u}} \odot \Phi_{\mathbf{r}}) \, (\mathbf{I} - \mathbf{\Omega}_r) \tag{4.24}$$

where $\mathbf{\Omega}_r = \left(\mathbf{I} + \sigma_e^2 \Phi_r^{-1} \mathbf{\Xi}_r\right)^{-1}$. Here, for $u = 1, \ldots, 2N$, $\mathbf{h}_u$, $\bar{\mathbf{h}}_u$ and $\mathbf{g}_u$ are the u-th columns of $\mathbf{H}$, $\overline{\mathbf{H}}$ and $\mathbf{G}$, respectively, and X_v denotes the v-th symbol in the constellation alphabet where $v = 1, \ldots, L$. In this formulation, $\wp_{u,u}$ is a $2N \times 2N$ matrix described as (u,u)-th sub-block of $vec\,(\mathbf{1}_{N\times M} \otimes \mathbf{\Gamma}_v) \, vec\,(\mathbf{1}_{N\times M} \otimes \mathbf{\Gamma}_v)^\dagger$.

$vec\,(\mathbf{1}_{N\times M} \otimes \mathbf{\Gamma}_v) \, vec\,(\mathbf{1}_{N\times M} \otimes \mathbf{\Gamma}_v)^\dagger$ is formed of $4M^2$ sub-matrices with size of $2N \times 2N$ and $\wp_{u,u}$ is the (u,u)-th sub-matrix. Correspondingly, the pairwise error probability of estimating $(\hat{u}, \hat{v})$ index pair instead of the (u,v) pair is shown as

$$P_s(u, \hat{u}, \psi_u, \psi_{\hat{u}}, v, \hat{v}) = \; Pr.\Big\{ D(u,v) > D(\hat{u},\hat{v}) \Big\} = Q\left(\sqrt{\frac{\|\mathbf{z}\|^2}{2}}\right) \tag{4.25}$$

where $\mathbf{z}$ is a complex Gaussian random vector with $2N \times 1$ dimension described as

$$\mathbf{z} = \mathbf{\Lambda}_{u,v}^{-\frac{1}{2}} \left(\mathbf{m}_{u,v} - \mathbf{m}_{\hat{u},\hat{v}}\right). \tag{4.26}$$

Notice that in general a closed-form solution for (4.25) does not exist for general modulations. However, for constellations with fixed envelope such as L-PSK where $|X_v| = c$ for all $v = 1, \ldots, L$, $\mathbf{\Lambda}_{u,v}$ becomes constant and the equation in (4.25) ensures the exact PEP for this modulation. In the case of constellations with a changing envelope, such as L-QAM, such a simplification is not possible. In this case an approximate,

but relatively close bound, can be obtained by using the assumption that $\mathbf{\Lambda}_{u,v} = \mathbf{\Lambda}_{\hat{u},\hat{v}}$. Notice that because most constellations are symmetric and also the covariance matrix $\mathbf{\Lambda}_{u,v}$ relies on the magnitude of symbols and not on the symbols itself, this approach results in a fairly close approximation. Notice that in the case of L-QAM the approximate PEP corresponds to the exact PEP of the mismatched ML detector employing the distance metric

$$D(u,v) = (\mathbf{y} - \mathbf{m}_{u,v})^{\dagger} \mathbf{\Lambda}_{u,v}^{-1} (\mathbf{y} - \mathbf{m}_{u,v}) \tag{4.27}$$

where the logarithm term is omitted. It is shown in [38] and [40] that $\mathbf{z}$ is a complex Gaussian vector as in the perfect estimation scenario, with mean vector and covariance matrix defined by following equations:

$$\mathbf{m_z} = \sqrt{\frac{K}{1+K}} \mathbf{\Lambda}_{u,v}^{-\frac{1}{2}} \left(\left(\mathbf{x}_{u,v}^T \mathbf{\Psi_{u,u}} - \mathbf{x}_{\hat{u},\hat{v}}^T \mathbf{\Psi}_{\hat{\mathbf{u}},\hat{\mathbf{u}}} \right) \otimes \mathbf{I} \right) vec\left(\bar{\mathbf{H}} \right) \tag{4.28}$$

$$\mathbf{\Lambda_z} = \frac{1}{K+1} \tilde{\mathbf{\Lambda}}_{u,v} \mathbf{\Theta} \tilde{\mathbf{\Lambda}}_{u,v}^{\dagger} \tag{4.29}$$

where $\tilde{\mathbf{\Lambda}}_{u,v}$ and $\mathbf{\Theta}$ terms in (4.29) can be derived as

$$\tilde{\mathbf{\Lambda}}_{u,v} = \mathbf{\Lambda}_{u,v}^{-\frac{1}{2}} \mathbf{\Omega}_r \mathbf{\Upsilon}(u, \hat{u}, \psi_u, \psi_{\hat{u}}, v, \hat{v}) \tag{4.30}$$

$$\mathbf{\Theta} = vec\left(\mathbf{1}_{N \times M} \otimes \mathbf{\Gamma}_v \right) vec\left(\mathbf{1}_{N \times M} \otimes \mathbf{\Gamma}_v \right)^{\dagger} \odot \left(\Phi + \sigma_e^2 \mathbf{\Xi} \right) \tag{4.31}$$

and

$$\mathbf{\Upsilon}(u, \hat{u}, \psi_u, \psi_{\hat{u}}, v, \hat{v}) = (\mathbf{x}_{u,v}^T \mathbf{\Psi_{u,u}} - \mathbf{x}_{\hat{u},\hat{v}}^T \mathbf{\Psi}_{\hat{\mathbf{u}},\hat{\mathbf{u}}}) \otimes \mathbf{I} \tag{4.32}$$

with $\Phi = \Phi_t^T \otimes \Phi_r$ and $\mathbf{\Xi} = \mathbf{\Xi}_t^T \otimes \mathbf{\Xi}_r$.

Then, after the computations of the mean vector and covariance matrix of the $\mathbf{z}$ vector is done, they can be used to find a closed form equation for the APEP's and the ABEP might be approximated by following the equations shown through (4.7)-(4.13).

4.3. Precoder optimization for minimum ABEP

The transmitter is considered to have partial information about the channel and the spatial correlation quality among transmit antennas, but because there is no complete information about the slow-fading channel we can not do a channel aware optimization for the precoder. A preferable attempt can be minimizing the ABEP upper-bound as shown in (4.7) at enough high SNR values. Our attempt for the proposed work is finding the optimum phase rotation values utilizing numerical search methods on the spaces of phase coefficients.

To demonstrate how the optimum phase rotation values, which are coming from the minimization of the average bit error probability upper bound, are identified and to illustrate its effect on the simulated ABER performance over Rayleigh and Rician channels, we first assume 2×2 DP-SM MIMO systems which are employing different constellations to convey information. For these systems, the symbols are sent from the first polarization of the first antenna with no rotation ($\theta_1 = 0$), and the symbols coming from other polarizations are rotated with θ_2, θ_3 and θ_4 respectively. Therefore three optimum phase parameters are required to be estimated. In all situations, $\mathbf{\Sigma_r} = \mathbf{I}$ is supposed, because the correlation at the receiver side does not affect our precoder design. In all cases the fixed component of the channel is assumed as an all one matrix to simplify the modeling. In all simulations and theoretical results shown in this work, all dual-polarized antennas used at transmitter and receiver are supposed to have the equal polarization representatives, so XPD parameters are assumed as $\chi_f = 15$dB and $\chi_v = 5$dB for fixed and variable components respectively. Furthermore components of the transmitter and receiver are supposed to be equal; consequently $\gamma_t = \gamma_r = \gamma$. The ABER curves for DP-SM MIMO systems are got for $\gamma = 0$ values. In Rician fading case, $K = 3$ is assumed. Besides, perfect and also imperfect channel estimations are considered both in all simulations and theoretical bounds. For the imperfect channel estimation scenario, Gaussian estimation errors are taken into account with mean of zero and constant variance of $\sigma_e^2 = 0.01$. By supposing that the estimation errors for

channel coefficients are exposed to equal transmit and receive spatial correlations, also various forms are simple. The optimum values for phase rotation coefficients are measured at 24 dB SNR, because theoretical result are very close to the simulation results. Different θ values are obtained for various α_t values for Rayleigh and Rician fading channels. For a 2×2 DP-SM system employing BPSK and QPSK the three optimum values for θ_l where $l = 2, 3, 4$ are selected from the range $[0, \pi]$ and $[0, \pi/2]$ respectively. In all cases the optimum values for rotation angles are different from each other and also this values are dependent to the correlation coefficient at the transmitter side. For DP-SM systems working at high spectral efficiencies, we have to use large numbers of transmit antenna arrays and/or higher order constellations. For this part of work we assume a 2×2 DP-SM system employing 8PSK and 16-QAM, and also a 4×2 DP-SM system employing QPSK and 8-QAM. Optimum values for phase rotation amounts are shown for different systems and constellation schemes in the following tables.

Table 4.1. Optimum precoding values for 2×2 DP-SM employing BPSK for Rayleigh channel.

α_t	θ_1	θ_2	θ_3	θ_4
0.99	0	0.06π	0.48π	0.54π
0.9	0	0.06π	0.48π	0.54π
0.8	0	0.02π	0.47π	0.49π
0.7	0	0.01π	0.47π	0.48π
0.5	0	0.49π	0.45π	0.04π

Table 4.2. Optimum phase rotation values for 2×2 DP-SM employing BPSK for Rician channel.

α_t	θ_1	θ_2	θ_3	θ_4
0.99	0	0.17π	0.48π	0.64π
0.9	0	0.17π	0.48π	0.65π
0.8	0	0.17π	0.48π	0.65π
0.7	0	0.17π	0.48π	0.65π
0.5	0	0.17π	0.48π	0.65π
0	0	0.17π	0.48π	0.65π

Table 4.3. Optimum precoding values for 2×2 DP-SM employing QPSK for Rayleigh channel.

α_t	θ_1	θ_2	θ_3	θ_4
0.99	0	0.4π	0.24π	0.16π
0.9	0	0.27π	0.23π	0.04π
0.8	0	0.02π	0.22π	0.24π
0.7	0	0.34π	0.21π	0.13π
0.5	0	0.31π	0.16π	0.15π

Table 4.4. Optimum precoding values for 2×2 DP-SM employing QPSK for Rician channel.

α_t	θ_1	θ_2	θ_3	θ_4
0.99	0	0	0.24π	0.24π
0.9	0	0	0.24π	0.24π
0.8	0	0	0.24π	0.24π
0.7	0	0	0.24π	0.24π
0.5	0	0	0.23π	0.23π
0	0	0	0.22π	0.22π

Table 4.5. Optimum precoding values for 2×2 system with higher order constellations for $\alpha_t = 0.9$.

System and constellation	θ_1	θ_2	θ_3	θ_4
2×2 8PSK, Rayleigh channel	0	0.11π	0.1π	0.01π
2×2 8PSK, Rician channel	0	0	0.12π	0.12π
2×2 16QAM, Rayleigh channel	0	0.25π	0.22π	0.13π
2×2 16QAM, Rician channel	0	0	0.14π	0.14π

Table 4.6. Optimum precoding values for 4×2 system with $\alpha_t = 0.9$.

System,constellation	θ_1	θ_2	θ_3	θ_4	θ_5	θ_6	θ_7	θ_8
4×2 QPSK, Rayleigh	0	0.3π	0.24π	0.1π	0	0.4π	0.22π	0.2π
4×2 QPSK, Rician	0	0	0.35π	0.27π	0.13π	0.12π	0.24π	0.36π
4×2 8-QAM, Rayleigh	0	0.76π	0.22π	π	0.45π	0.76π	0.22π	π
4×2 8-QAM, Rician	0	0.03π	0.16π	0.16π	0.25π	0.25π	0	0.1π

4.4. Simulation Results

In this part of work, the impacts and benefits of the precoding scheme is shown, for Rayleigh and Rician fading and also for perfect and for Gaussian error estimation scenarios. The theoretical ABEP upper bounds are also plotted in dashed lines for both conventional (where all symbols are transmitted without any rotation) and precoded DP-SM, just for two cases (for the clarity of the presentation), which are very close to the simulation results, especially in high SNR values.

4.4.1. Rayleigh Fading

Here, the simulation results for correlated Rayleigh fading channels are represented. In this scenario $K = 0$ is assumed and a 2×2 DP-SM system employing BPSK or QPSK transmissions is considered. The effects of precoding is shown for uncorrelated and correlated fading channel with various correlation coefficients at the transmitter side. Results are shown for both erroneous and perfectly estimated channels.

Figure (4.1) illustrates the ABER for the 2×2 DP-SM system with BPSK constellation, for perfect and erroneous channel estimation cases respectively. It is obvious from this figure that, for BPSK case, the ABER for the phase rotated precoding DP-SM system meets the no correlated DP-SM, independent of the transmit antenna spatial correlations, whilst conventional DP-SM bears a considerable performance degradation particularly in high correlations. Furthermore, for small correlation values at the transmit side, both the deterioration of the performance and enhancement caused by the rotation optimized aided precoding are also small. In figure 4.1.b, the same results can be obtained for erroneous channel estimation, and it can be seen that the per-

formance deterioration of the conventional DP-SM system can be satisfied remarkably by optimal phase rotation. Figure (4.2) shows the performance of the 2×2 DP-SM employing QPSK for perfect and imperfect channel estimates. As in the BPSK case the precoding approach improves the performance especially in higher correlations. For erroneous channel estimations, however the performance decreases in comparison to perfect estimates, but it is obvious that the performance improvement based on precoding is increased in comparison to perfect channel estimation.

4.4.2. Rician Fading

The advantages of the proposed precoding approach is more clear when the channel experiences LOS component (Rician fading effects) in addition to the high spatial correlations at the transmitter side. In order to show this effect, we present the effects of the rotation optimization on the average bit error rate with respect to SNR. In figures (4.3) and (4.4), the performances of the conventional and rotation optimized DP-SM systems performing in the correlated Rician fading cases for different transmit correlation coefficients are shown. where the constellations of BPSK and QPSK are used, respectively. All theoretical upper bounds are very close to the simulated ABER performances, however only two cases are shown for clearness of presentment. As shown in figure (4.3), for BPSK, performance of the precoded DP-SM system with rotated constellations, goes to a single ABER performance, freely of the correlation coefficients at the transmitter side.

It is obvious from this figure that for the uncorrelated transmit antennas ($\alpha_t = 0$), the precoding approach, improves the performance approximately 6 dB (for 10^{-5} BER level). The advantages of rotation-based precoding is more obvious when the correlation among antennas is high. The same results can be obtained from the erroneous channel estimation scenario. Figure (4.4) illustrates performance of the system for the same number of antennas employing QPSK. Similar to previous system, the deterioration in performance for the conventional DP-SM approach can be satisfied considerably by rotation optimized precoding.

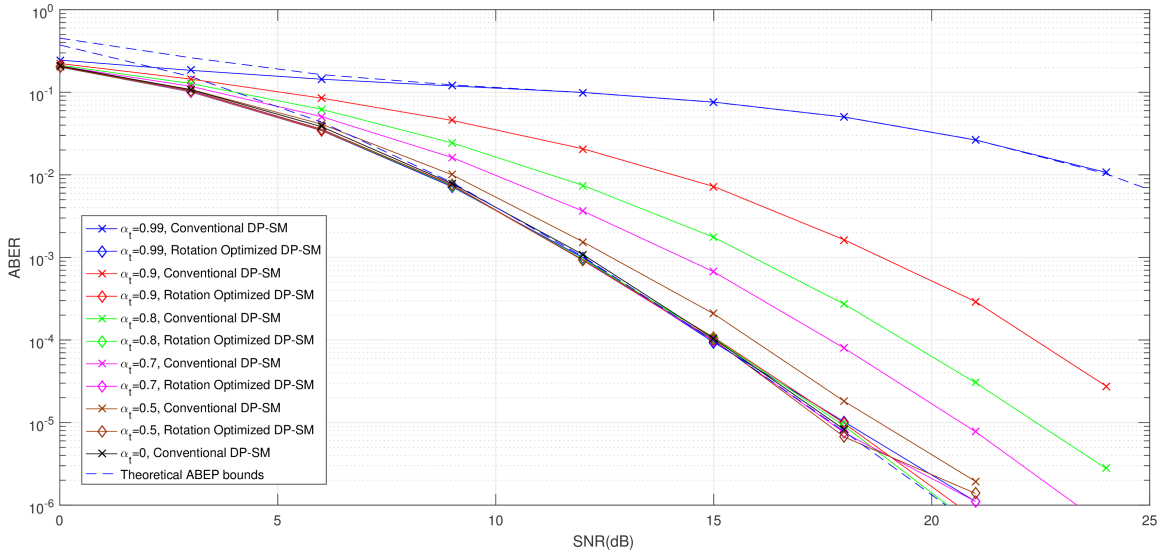

(a)

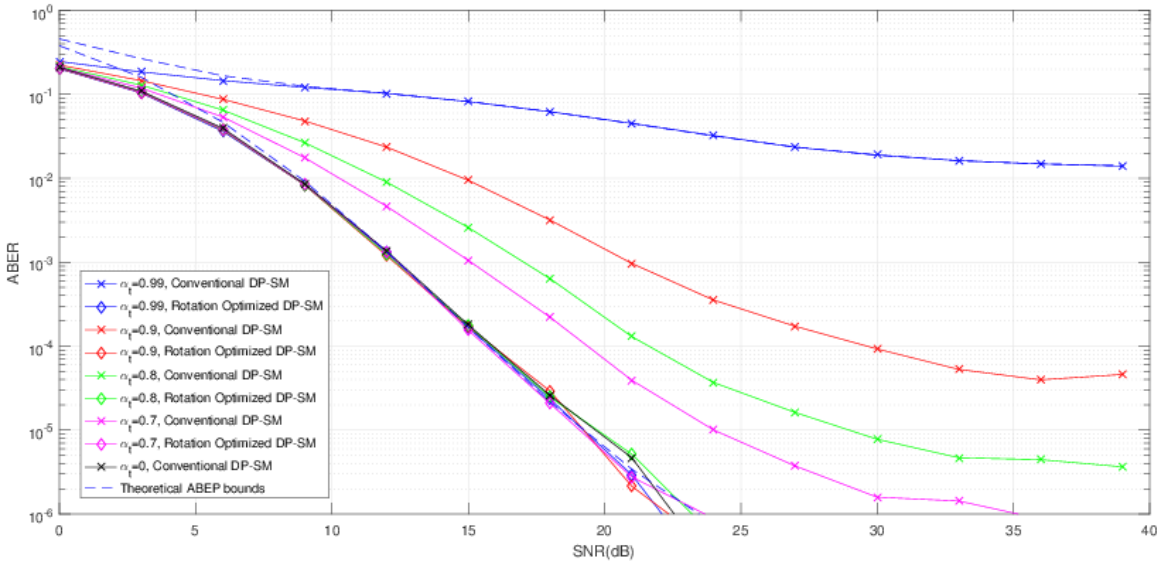

(b)

Figure 4.1. ABER comparison for rotation-optimized and conventional 2×2 DP-SM-MIMO systems employing BPSK over Rayleigh channel for, a) perfectly estimated channel, b) imperfectly estimated channel with variance $\sigma_e^2 = 0.01$.

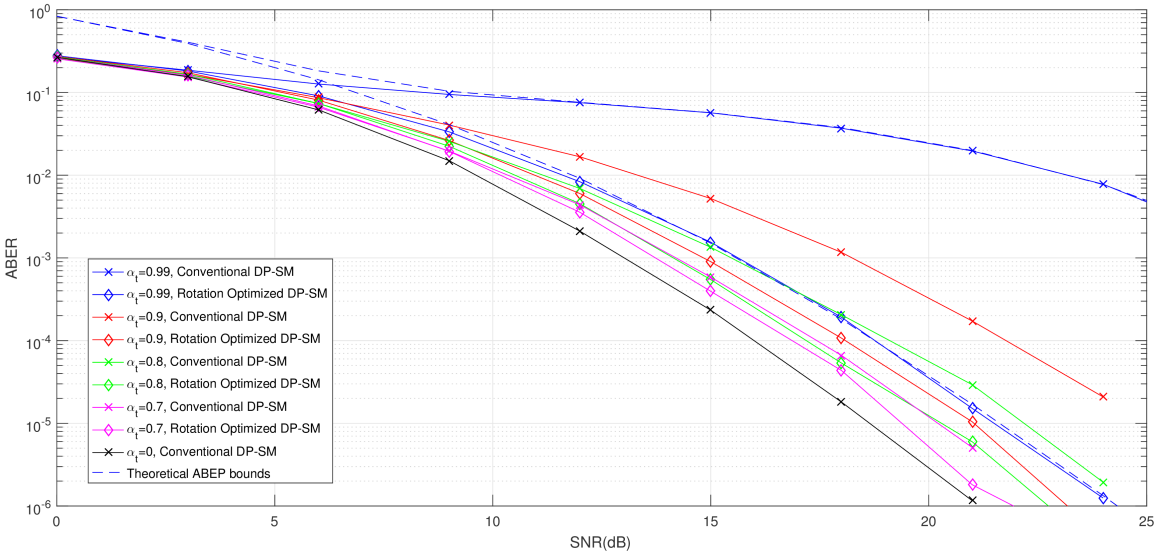

(a)

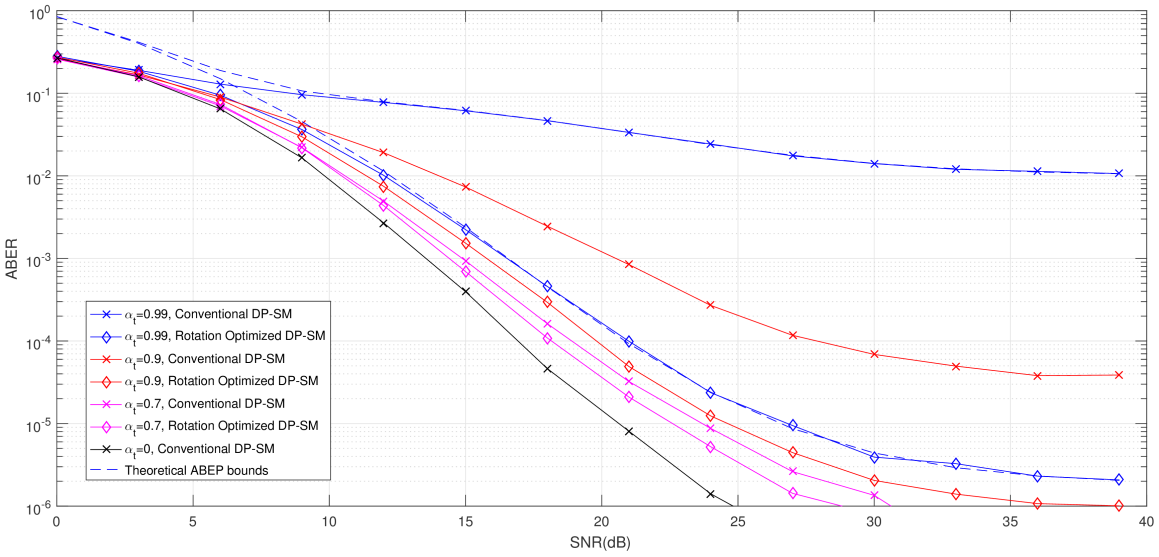

(b)

Figure 4.2. ABER comparison for rotation-optimized and conventional 2×2 DP-SM-MIMO systems employing QPSK over Rayleigh channel for, a) perfectly estimated channel, b) imperfectly estimated channel with variance $\sigma_e^2 = 0.01$.

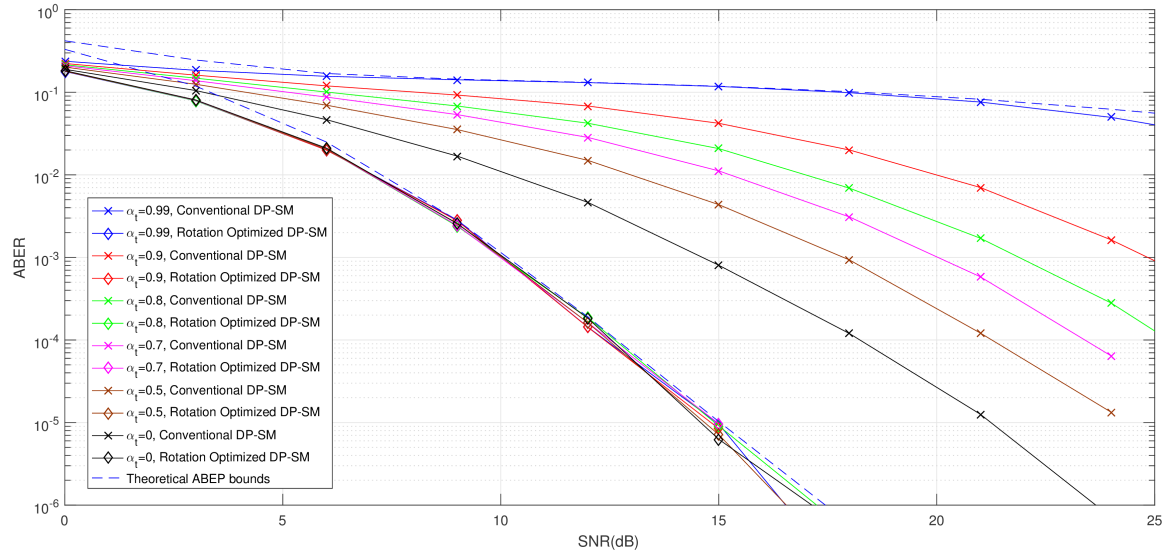

(a)

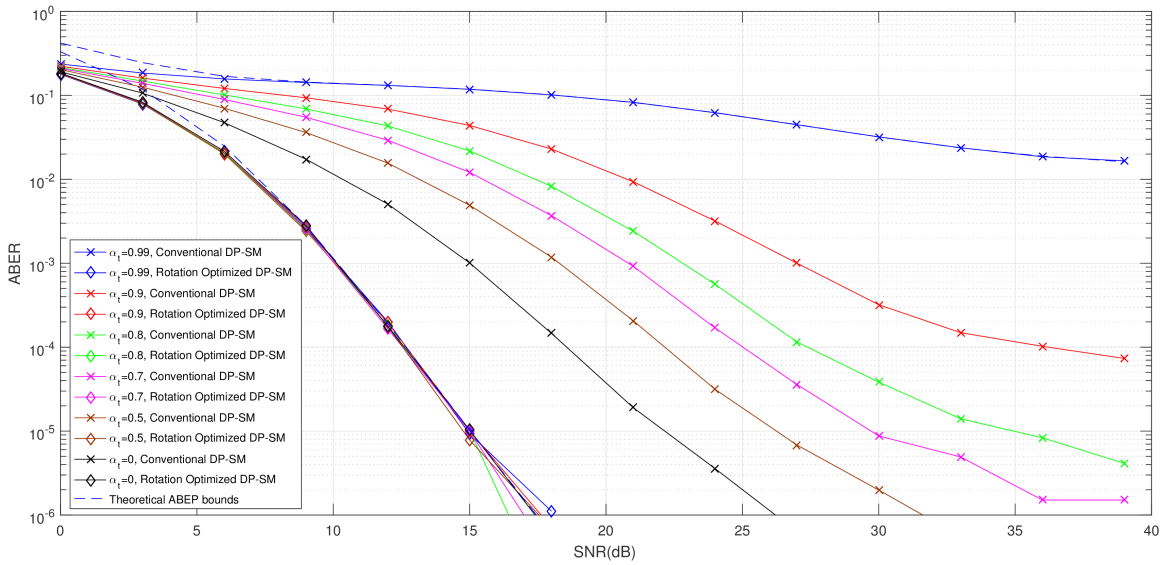

(b)

Figure 4.3. ABER comparison for rotation-optimized and conventional 2×2 DP-SM-MIMO systems employing BPSK over Rician channel for, a) perfectly estimated channel, b) imperfectly estimated channel with variance $\sigma_e^2 = 0.01$.

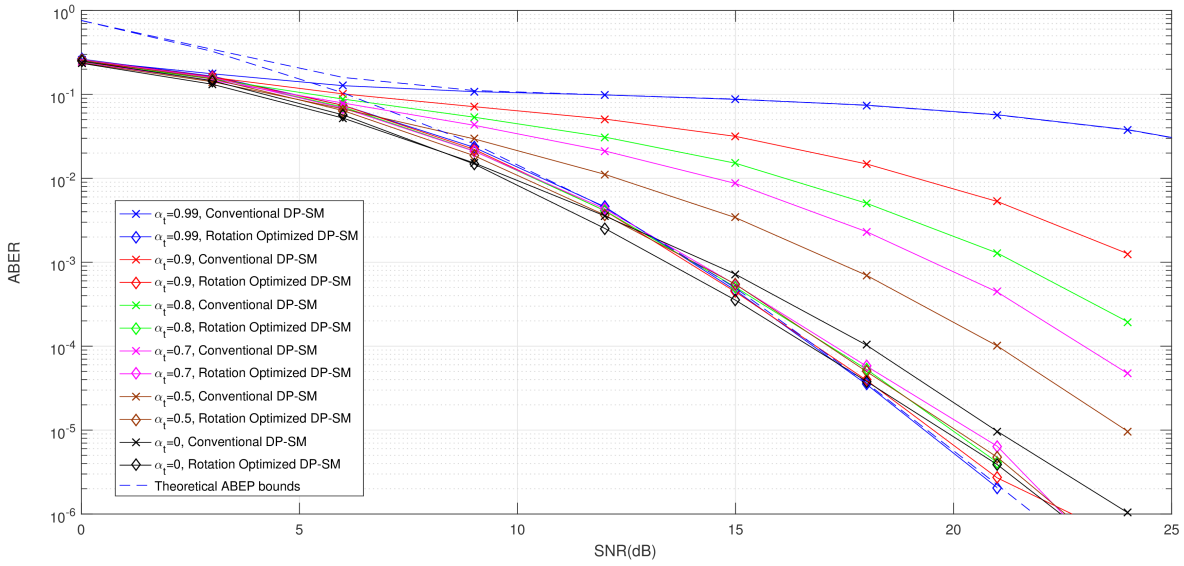

(a)

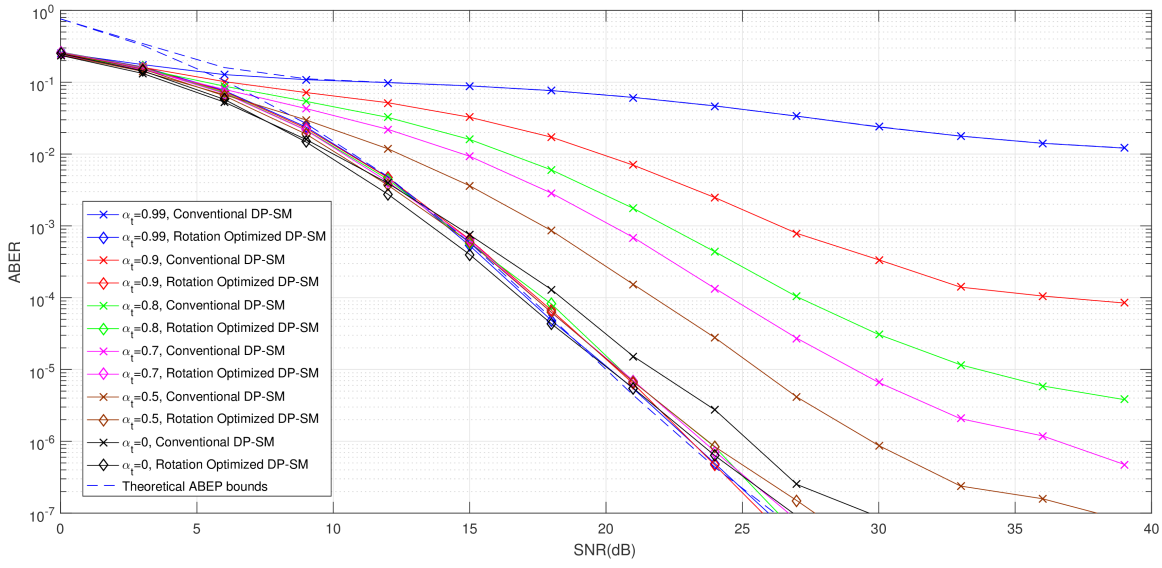

(b)

Figure 4.4. ABER for rotation-optimized and conventional 2×2 DP-SM-MIMO systems employing QPSK over Rician channel for, a) perfectly estimated channel, b) imperfectly estimated channel with variance $\sigma_e^2 = 0.01$.

4.4.3. Higher Order Systems and Modulations

In previous parts of the work, the potential benefits of the proposed precoding approach have been presented for small DP-SM systems with 2 transmit antennas, employing simple modulations such as BPSK and QPSK. So the spectral efficiency of the systems was 3 or 4 bpcu. Nevertheless, when DP-SM MIMO systems with large number of transmit antennas arrays and/or higher order constellations are considered, this makes the ABER minimizing design more complex due to the larger number of precoding parameters which must be optimized, and/or the increased number of APEP terms to compute in (4.7) for large constellation size. In this section, the benefits of the precoding scheme for DP-SM systems functioning at higher spectral efficiencies, (5 and 6 bpcu for this part of work are assumed) are presented in figures 4.5 and 4.6 respectively. Notice that higher spectral efficiencies may be obtained by using higher order constellations and/or more transmit antenna numbers. To achieve 5 bpcu spectral efficiency, we consider a 2×2 DP-SM system employing 8PSK and also a 4×2 DP-SM system employing QPSK. The ABER performances for these systems are shown in figure 4.5 for different fading channels. Similarly for spectral efficiency of 6 bpcu, we assume a 2×2 DP-SM with 16-QAM constellation and also a 4×2 DP-SM system utilizing 8-QAM modulation as in figure 4.6. Higher numbers of antennas at the transmitter side also constellation schemes are skipped for clearness of the figures. For simulated results, correlated non-line-of-sight and line-of-sight channels are supposed with correlation coefficient of $\alpha_t = 0.9$. For Rician fading, the Rician factor K, is assumed $K = 3$ as before. Similarly, the antennas at the receiver side are assumed to be uncorrelated ($\mathbf{\Sigma_r} = \mathbf{I}$). For all simulations in this part we assume the both channel estimations as perfect and erroneous with variance of $\sigma_e^2 = 0.01$ as before.

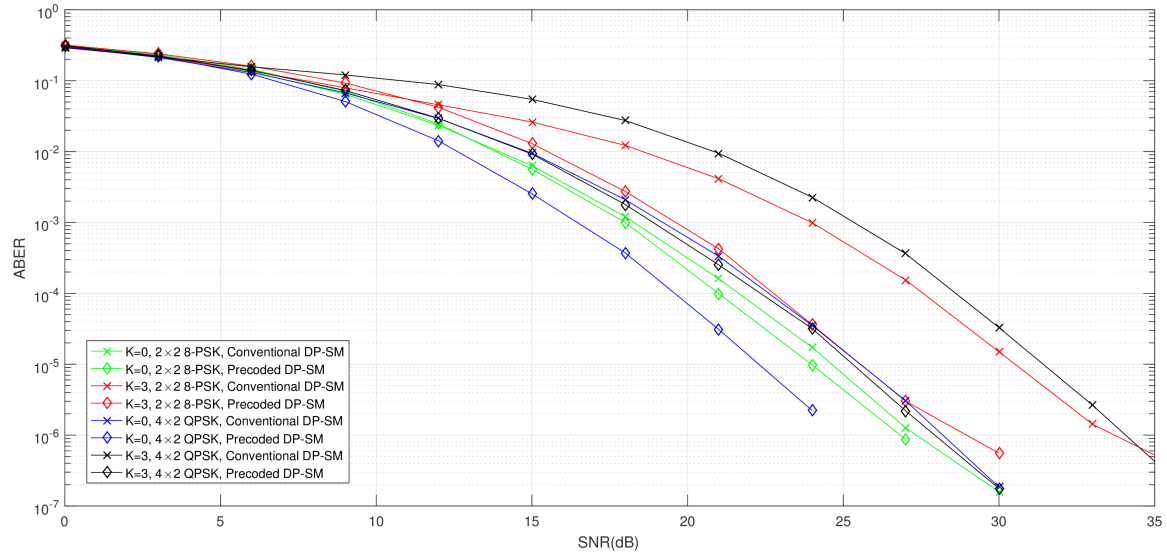

(a)

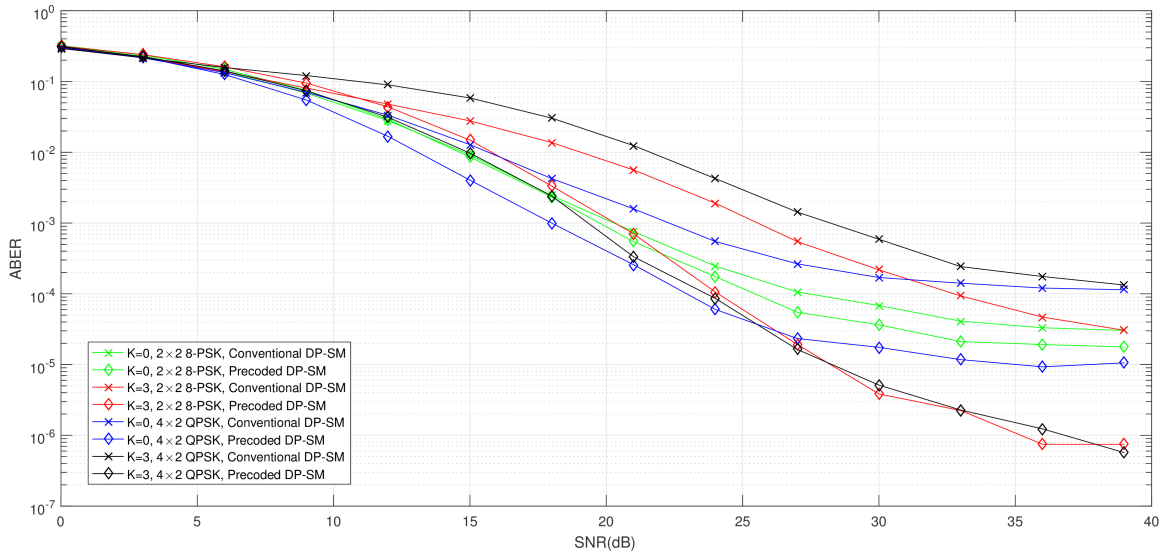

(b)

Figure 4.5. ABER for rotation-optimized and conventional DP-SM-MIMO systems with spectral efficiency of 5 bpcu over correlated channels fora) perfectly estimated channel, b) imperfectly estimated channel with variance $\sigma_e^2 = 0.01$.

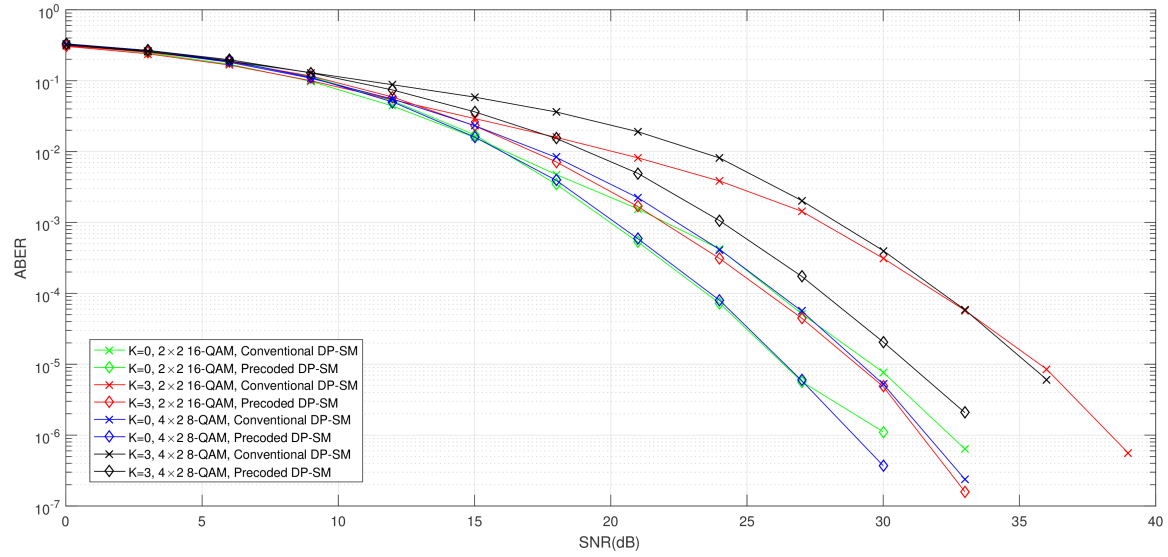

(a)

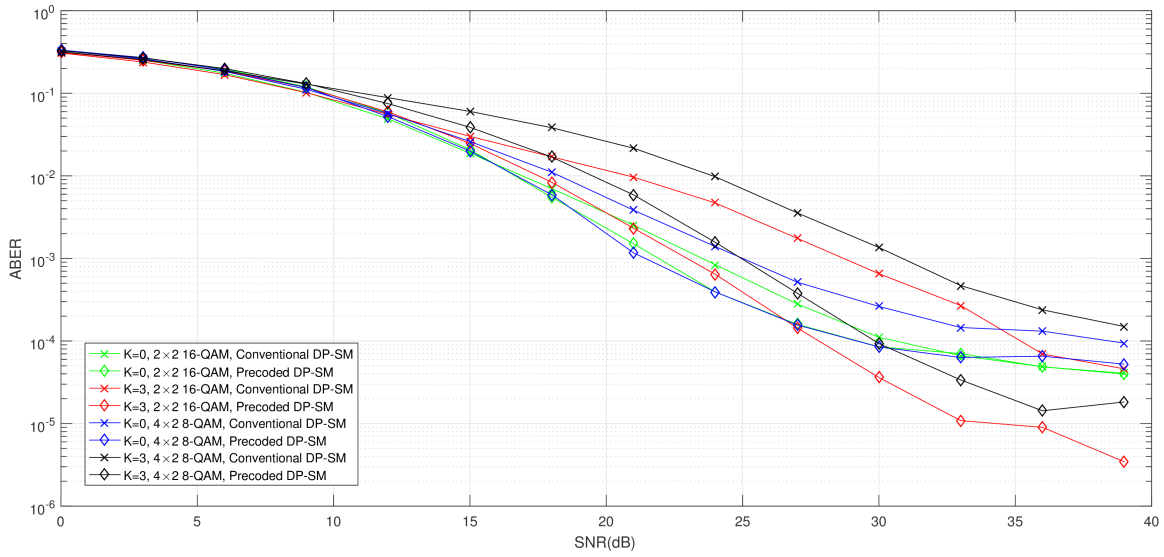

(b)

Figure 4.6. ABER for rotation-optimized and conventional DP-SM-MIMO systems with spectral efficiency of 6 bpcu over correlated channels for a) perfectly estimated channel, b) imperfectly estimated channel with variance $\sigma_e^2 = 0.01$.

4.4.4. Comparison with Precoded Uni-polarized-SM MIMO Systems

The next figures are displayed in order to show the comparison between precoded DP-SM and precoded UP-SM systems with the same spectral efficiencies over different fading channels for perfect and imperfect channel estimations. As it is shown in figures, all theoretical ABEP upper bounds are very close to simulation results. The results are shown for Rayleigh and Rician fading channels respectively. Because of the space limitations the comparison is just done for high correlation coefficient $\alpha_t = 0.9$. In this part the comparison among rotation optimized 2×2 dual-polarized SM system and rotation optimized 2×2 and 4×4 uni-polarized SM systems (which are shown completely in [26]) is done, and all systems are simulated for 3 and 4 bpcu spectral efficiencies.

Notice from figure 4.7, for the correlated Rayleigh, precoded 2×2 DP-SM system employing BPSK excels 2×2 UP-SM system which employs QPSK, by 12 dB (at 10^{-5}) and performs 1 dB worse than the precoded 4×4 UP-SM system using BPSK constellation, whereas it uses half as much space. As it is shown in figure 4.7.b, in correlated Rayleigh channel with Gaussian estimation errors, precoded 2×2 DP-SM system works approximately 12 dB (at 10^{-5}) better than 2×2 UP-SM system and has better performance than equivalent precoded 4×4 UP-SM system at large SNR values. This result comes from the robustness of dual-polarized SM systems against channel estimation errors. In figure 4.8, a precoded 2×2 DP-SM system employing BPSK is assumed and it is compared to the precoded 2×2 and 4×4 UP-SM systems with constellations of QPSK and BPSK respectively, over correlated Rician fading channels. It is illustrated that in correlated Rician, rotation optimized 2×2 DP-SM system works better than 2×2 UP-SM system with the same spectral efficiency by 10 dB (at 10^{-5}) and has almost the same performance as equivalent precoded 4×4 UP-SM system while employing half as much space. As it is obvious DP-SM systems perform better in erroneous channel estimation case because they are more strong toward the channel corruptions such as Rician fading effects and spatial correlation among antennas in addition to channel estimation errors comparing with UP-SM systems.

The next figures are displayed in order to compare rotation optimized 2×2 dual-polarized SM system with rotation optimized 2×2 and 4×4 uni-polarized SM systems (which are shown completely in [26]) with spectral efficiency of 4b/s/Hz in different fading channel scenarios. In Fig. 4.9, a precoded 2×2 DP-SM system is shown with spectral efficiency of 4 bpcu (using QPSK modulation) and compared with the rotation optimized 2×2 and 4×4 UP-SM systems (using 8-PSK and QPSK constellations, respectively). As shown all theoretical ABEP upper bounds are close to the simulated performances. The results are shown for perfect and imperfect channel estimations in Fig. 4.9 (a) and (b) respectively. Because of the space limitation we just do the comparison for $\alpha_t = 0.9$. Notice from Fig. 4.9 (a), for correlated Rayleigh, precoded 2×2 DP-SM system shows better performance than its 2×2 UP-SM counterpart by 10 dB (at 10^{-4}) and performs only 1 dB worse than the equivalent precoded 4×4 UP-SM system while using half of its space. In Fig. 4.9 (b) we can see that in erroneous channel estimation case precoded 2×2 DP-SM system excels its 4×4 UP-SM at large SNR values and this result shows that DP-SM systems are considerably more resistant toward spatial correlations as well as imperfect channel estimation in comparison to UP-SM systems. In figure 4.10, it can be seen that in the correlated Rician channel, precoded 2×2 DP-SM system has better performance than 2×2 and precoded 4×4 UP-SM counterparts by 12 dB and 1 dB (at 10^{-5}) differences, respectively. In Fig. 4.10 (b), for imperfect channel estimation scenario, it is illustrated that the gap between precoded DP-SM system and its counterpart rotation-optimized UP-SM systems is increased especially in high SNR values as in the Rayleigh fading case.

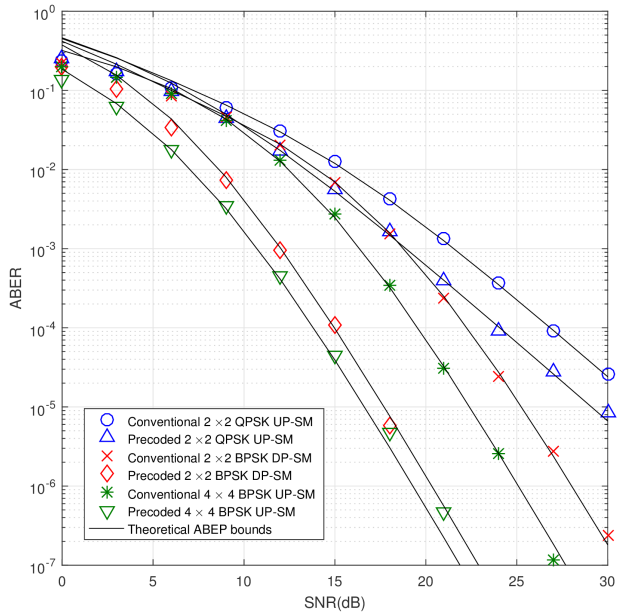

(a)

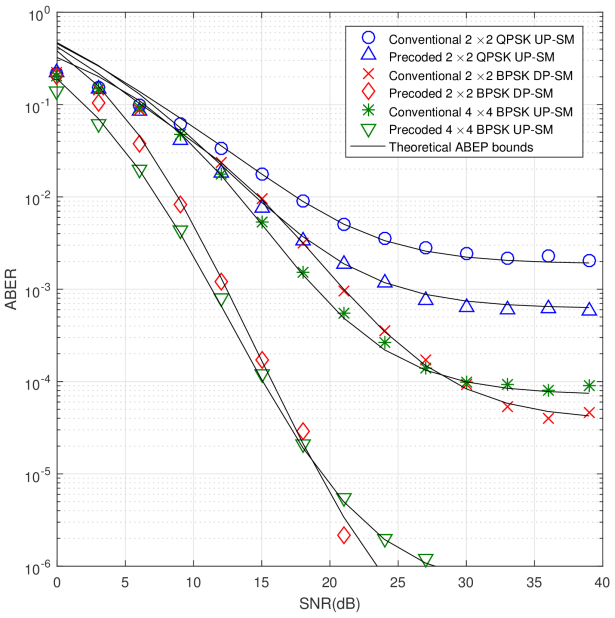

(b)

Figure 4.7. ABER comparison for 2×2 DP-SM-MIMO systems with 2×2 and 4×4 UP-SM with R=3 b/s/Hz and $\alpha_t = 0.9$ over Rayleigh channel for a) perfectly estimated channel, b) imperfectly estimated channel with variance $\sigma_e^2 = 0.01$.

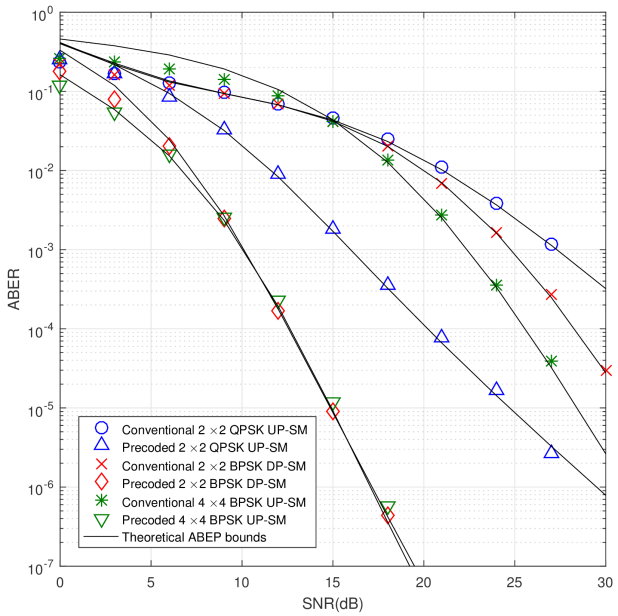

(a)

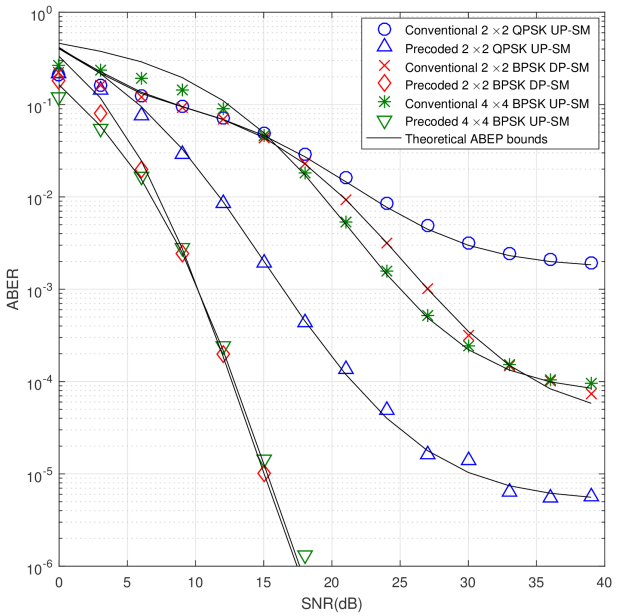

(b)

Figure 4.8. ABER comparison for 2×2 DP-SM-MIMO systems with 2×2 and 4×4 UP-SM with R=3 b/s/Hz and $\alpha_t = 0.9$ over Rician channel for a) perfectly estimated channel, b) imperfectly estimated channel with variance $\sigma_e^2 = 0.01$.

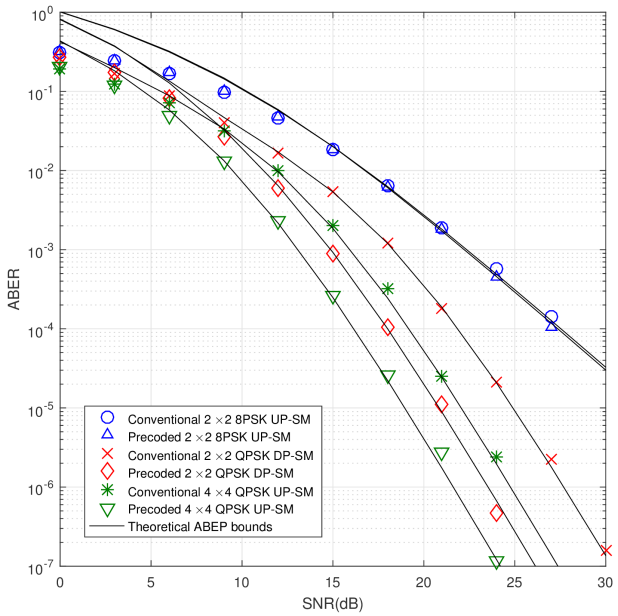

(a)

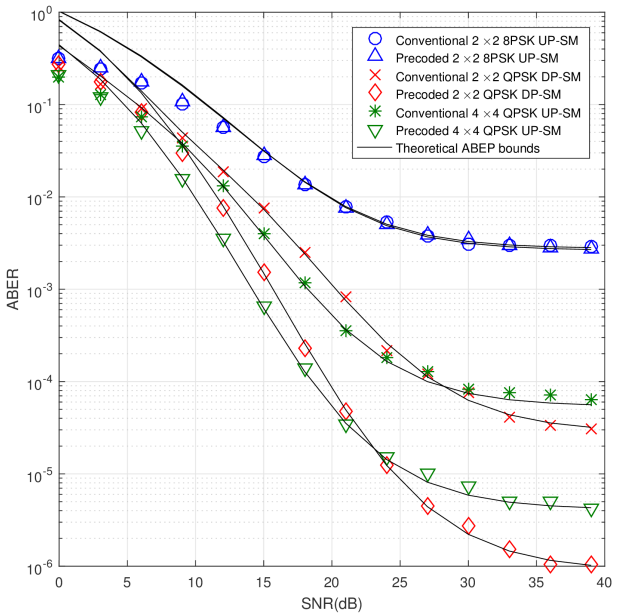

(b)

Figure 4.9. ABER comparison of 2×2 DP-SM-MIMO systems with 2×2 and 4×4 UP-SM with R=4 b/s/Hz and $\alpha_t = 0.9$ over Rayleigh channel for a) perfectly estimated channel, b) imperfectly estimated channel with variance $\sigma_e^2 = 0.01$.

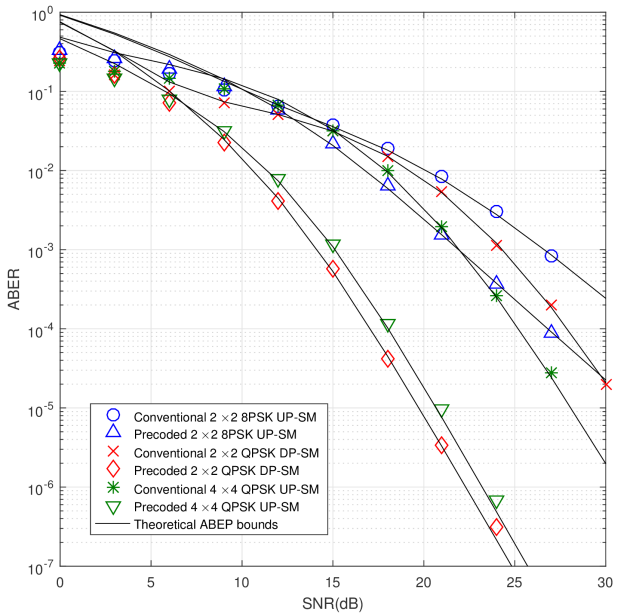

(a)

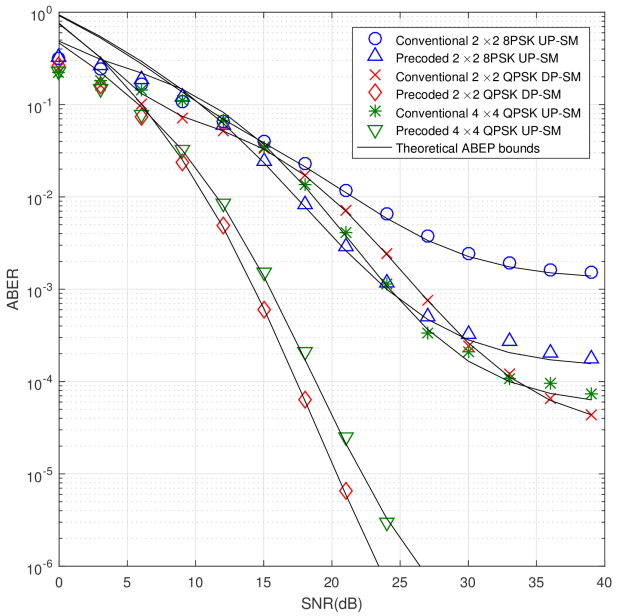

(b)

Figure 4.10. ABER comparison of 2×2 DP-SM-MIMO systems with 2×2 and 4×4 UP-SM with R= b/s/Hz and $\alpha_t = 0.9$ over Rician channel for a) perfectly estimated channel, b) imperfectly estimated channel with variance $\sigma_e^2 = 0.01$.

4.5. Unequal Error Protection

It is assumed, in classical theoretical framework, that all information in communication is equally important as in [41], so that any particular message being mistaken is viewed to be equally costly, as any other. With this assumption, reliability of a system is measured by the average probability of the error, over all possible messages which are being transmitted. Another advantage of the average bit-error rate upper bounding approach shown throughout the work, is letting to characterize the unequal error protection need of DP-SM system. The respective upper bounds for the average bit-error probability of antenna and the symbol bits can be written as below respectively:

$$\bar{P}_b^a \leq \frac{1}{2ML} \sum_{u=1}^{2M} \sum_{\hat{u}=1}^{2M} \sum_{v=1}^{L} \sum_{\hat{v}=1}^{L} \frac{N(u,\hat{u})}{\log_2(2M)} \bar{P}_s(u,\hat{u},\psi_u,\psi_{\hat{u}},v,\hat{v}) \tag{4.33}$$

$$\bar{P}_b^s \leq \frac{1}{2ML} \sum_{u=1}^{2M} \sum_{\hat{u}=1}^{2M} \sum_{v=1}^{L} \sum_{\hat{v}=1}^{L} \frac{N(v,\hat{v})}{\log_2(L)} \bar{P}_s(u,\hat{u},\psi_u,\psi_{\hat{u}},v,\hat{v}) \tag{4.34}$$

where $N(u,\hat{u})$ is the bit error numbers among respective indices of the u-th and $\hat{u}$-th unique active transmit antenna and polarization direction pair. $N(v,\hat{v})$ is the bit error numbers between the indices of the v-th and $\hat{v}$-th symbols in the modulation alphabet. As it is obvious that $N(u,\hat{u},v,\hat{v}) = N(u,\hat{u}) + N(v,\hat{v})$, it is straightforward to show that:

$$\bar{P}_b = \frac{\bar{P}_b^a}{\log_2(L)} + \frac{\bar{P}_b^s}{\log_2(2M)}. \tag{4.35}$$

Once the APEP's in (4.13) are calculated, $\bar{P}_b^a$ and $\bar{P}_b^s$ can also be obtained conveniently and as they are in tight agreement especially for high SNR values with the simulated results, the ratio of $\bar{P}_b^a/\bar{P}_b^s$ (or $\bar{P}_b^s/\bar{P}_b^a$) is utilized as a metric to measure how the channel impairments such as correlation at the transmitter side and/or Rician affect different bits unequally. In order to represent this, we plot the $\bar{P}_b^a/\bar{P}_b^s$ curves for conventional and also precoded 2×2 DP-SM system in figure 5.11. By considering BPSK and QPSK constellations, for Rayleigh and Rician fading channels. Theoretical average bit error

probabilities are computed at SNR of 24 dB and are plotted with respect to different α_t values at the transmitter side. $\alpha_t = 0$ corresponds to fully uncorrelated transmit antennas and $\alpha_t = 1$ shows the fully correlated scenario. In figure 5.11, conventional DP-SM theoretical average bit-error probabilities are illustrated with dashed lines, whereas precoded ones are presented with solid lines. As previous parts, uncorrelated antennas ($\mathbf{\Sigma_r} = \mathbf{I}$) is assumed for the receiver side.

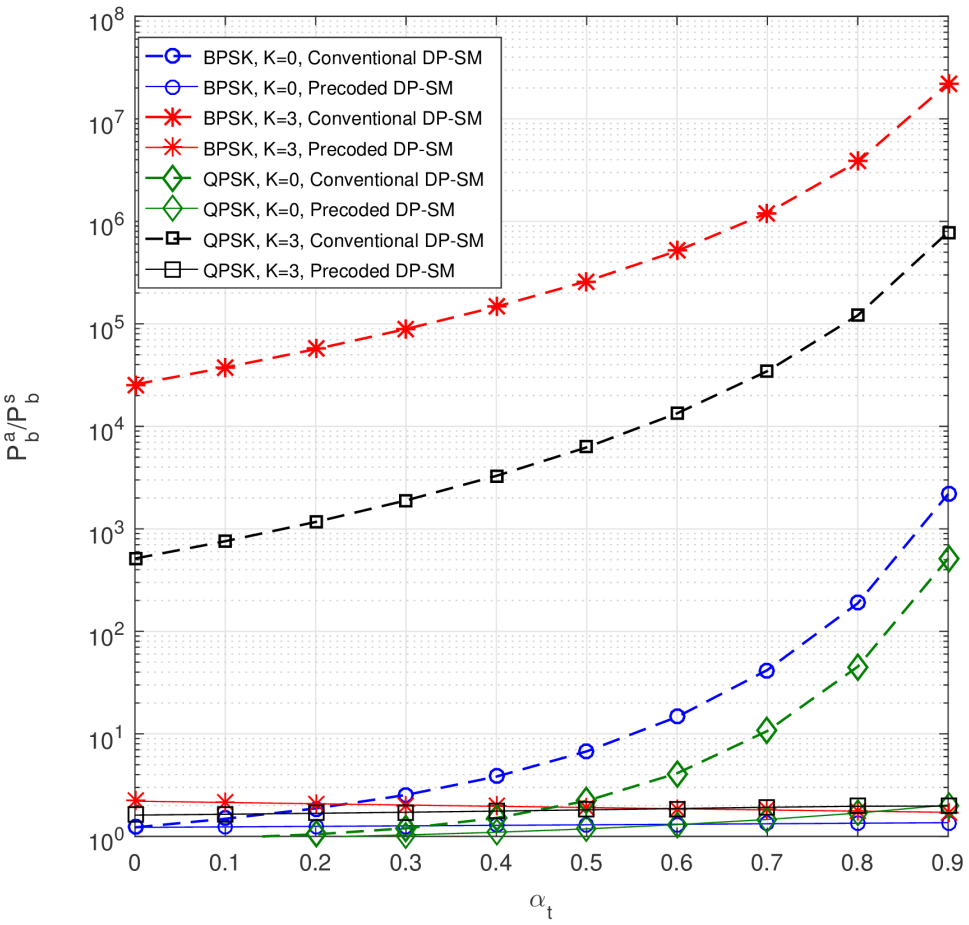

Figure 4.11. Antenna Bit ABER/Symbol Bit ABER comparisons of conventional and optimally precoded 2×2 dimensional DP-SM system.

For the Rayleigh fading case, when the transmitter antennas are uncorrelated or for small correlation coefficient values, the ABEP values for symbol and antenna cases are nearly the same. Nevertheless as the correlation coefficient increases and the spatial correlation affects the information bits more, the antenna bits are affected more

than the symbol bits. So, $\bar{P}_b^a/\bar{P}_b^s$ is increasing with α_t as it is shown in figure. For Rician channels, with the assumption of $K = 3$, the ratio is large even for uncorrelated transmit antennas and also it is increasing to very large values with increasing α_t. The need for unequal error protection is obvious for both cases. At the other side, when the precoding is done for transmitted symbols with phase rotations, this makes the ratios of $\bar{P}_b^a/\bar{P}_b^s$ flat and close to unity in addition to the performance improvements as were shown in previous results. So, in conclusion, linear precoding decreases the requirement for protecting the information bits to be affected unequally and also removes the complex transceiver designs as in [19–22].

5. CONCLUSION

In this thesis we have discussed the effects of the precoding approach for dual-polarized spatial modulation systems over slow-fading correlated channels. The optimum rotation values are calculated by minimizing ABEP upper bound at large SNR values. Both simulation and analysis results indicate considerable enhancement over conventional DP-SM, where only minor increment for complexity of the computations is needed at the transmitter side. In general the correlated Rician channel model is presented, where uncorrelated and Rayleigh channels are the special cases of this model, by using the well-known Kronecker model.

By assuming perfect channel estimation, PEP, APEP and ABEP are derived and the optimum values of the precoding coefficients which minimize ABEP have been calculated. Then by using the optimum values we compare the error performance of the conventional DP-SM system with the proposed precoded DP-SM system in different channel cases and also various correlation coefficient values at the transmitter side, in order to find out the advantages of the precoding scheme especially for highly correlated systems in addition to Rician fading effects. Second we have analyzed the performance of the system for the case where the channel estimation error is present. For this case, the theoretical ABEP analysis is an exact result for M-PSK and it is a close approximation for M-QAM. We use the same optimum values of the precoding matrix which have been founded for the perfect channel estimations. Comparing with the perfect channel estimates, due to the estimation error, a performance degradation is obvious from the results.

Over and above, we have presented that the rotation-optimized precoding approach combats significantly against the unequal error effects of the channel impairments on the antenna index and the symbol bits especially in high transmit antenna correlation and/or Rician fading, and eliminate the requirement for implementing complicated systems to achieve unequal error protection.

REFERENCES

1. Wolniansky, P. W., G. J. Foschini, G. Golden and R. A. Valenzuela, "V-BLAST: An architecture for realizing very high data rates over the rich-scattering wireless channel", *Signals, Systems, and Electronics, 1998. ISSSE 98. 1998 URSI International Symposium on*, pp. 295–300, IEEE, 1998.

2. Gesbert, D., M. Shafi, D.-s. Shiu, P. J. Smith and A. Naguib, "From theory to practice: An overview of MIMO space-time coded wireless systems", *IEEE Journal on selected areas in Communications*, Vol. 21, No. 3, pp. 281–302, 2003.

3. Torlak, M. and T. M. Duman, "MIMO communication theory, algorithms, and prototyping", *Signal Processing and Communications Applications Conference (SIU), 2012 20th*, pp. 1–2, IEEE, 2012.

4. Mesleh, R. Y., H. Haas, S. Sinanovic, C. W. Ahn and S. Yun, "Spatial modulation", *IEEE Transactions on Vehicular Technology*, Vol. 57, No. 4, pp. 2228–2241, 2008.

5. Jeganathan, J., A. Ghrayeb and L. Szczecinski, "Spatial modulation: Optimal detection and performance analysis", *IEEE Communications Letters*, Vol. 12, No. 8, 2008.

6. Di Renzo, M., D. De Leonardis, F. Graziosi and H. Haas, "Space shift keying (SSK—) MIMO with practical channel estimates", *IEEE Transactions on Communications*, Vol. 60, No. 4, pp. 998–1012, 2012.

7. Handte, T., A. Muller and J. Speidel, "BER analysis and optimization of generalized spatial modulation in correlated fading channels", *Vehicular Technology Conference Fall (VTC 2009-Fall), 2009 IEEE 70th*, pp. 1–5, IEEE, 2009.

8. ElKalagy, A. and E. AlSusa, "A novel spatial modulation technique with interference free simultaneous transmission", *Personal Indoor and Mobile Radio Communications (PIMRC), 2010 IEEE 21st International Symposium on*, pp. 809–814,

ieee, 2010.

9. Younis, A., N. Serafimovski, R. Mesleh and H. Haas, "Generalised spatial modulation", *Signals, Systems and Computers (ASILOMAR), 2010 Conference Record of the Forty Fourth Asilomar Conference on*, pp. 1498–1502, IEEE, 2010.

10. Wang, J., S. Jia and J. Song, "Generalised spatial modulation system with multiple active transmit antennas and low complexity detection scheme", *IEEE Transactions on Wireless Communications*, Vol. 11, No. 4, pp. 1605–1615, 2012.

11. Basar, E., U. Aygolu, E. Panayirci and H. V. Poor, "Space-time block coded spatial modulation", *IEEE Transactions on Communications*, Vol. 59, No. 3, pp. 823–832, 2011.

12. Erceg, V., P. Soma, D. S. Baum and S. Catreux, "Multiple-input multiple-output fixed wireless radio channel measurements and modeling using dual-polarized antennas at 2.5 GHz", *IEEE transactions on Wireless Communications*, Vol. 3, No. 6, pp. 2288–2298, 2004.

13. Soma, P., D. S. Baum, V. Erceg, R. Krishnamoorthy and A. Paulraj, "Analysis and modeling of multiple-input multiple-output (MIMO) radio channel based on outdoor measurements conducted at 2.5 GHz for fixed BWA applications", *Communications, 2002. ICC 2002. IEEE International Conference on*, Vol. 1, pp. 272–276, IEEE, 2002.

14. Oestges, C., V. Erceg and A. J. Paulraj, "Propagation modeling of MIMO multipolarized fixed wireless channels", *IEEE transactions on vehicular technology*, Vol. 53, No. 3, pp. 644–654, 2004.

15. Sellathurai, M., P. Guinand and J. Lodge, "Space-time coding in mobile satellite communications using dual-polarized channels", *IEEE Transactions on Vehicular Technology*, Vol. 55, No. 1, pp. 188–199, 2006.

16. Kyritsi, P., D. C. Cox, R. A. Valenzuela and P. W. Wolniansky, "Effect of antenna polarization on the capacity of a multiple element system in an indoor environ-

ment", *IEEE Journal on Selected areas in Communications*, Vol. 20, No. 6, pp. 1227–1239, 2002.

17. Zafari, G., M. Koca and H. Sari, "Dual-polarized spatial modulation over correlated fading channels", *IEEE Transactions on Communications*, Vol. 65, No. 3, pp. 1336–1352, 2017.

18. Bolcskei, H., R. U. Nabar, V. Erceg, D. Gesbert and A. J. Paulraj, "Performance of spatial multiplexing in the presence of polarization diversity", *Acoustics, Speech, and Signal Processing, 2001. Proceedings.(ICASSP'01). 2001 IEEE International Conference on*, Vol. 4, pp. 2437–2440, IEEE, 2001.

19. Mesleh, R., M. Di Renzo, H. Haas and P. M. Grant, "Trellis coded spatial modulation", *IEEE Transactions on Wireless Communications*, Vol. 9, No. 7, pp. 2349–2361, 2010.

20. Koca, M. and H. Sari, "Bit-interleaved coded spatial modulation", *Personal Indoor and Mobile Radio Communications (PIMRC), 2012 IEEE 23rd International Symposium on*, pp. 1949–1954, IEEE, 2012.

21. Yang, Z., C. Liang, X. Xu and X. Ma, "Block Markov superposition transmission with spatial modulation", *IEEE Wireless Communications Letters*, Vol. 3, No. 6, pp. 565–568, 2014.

22. Basar, E., U. Aygolu, E. Panayirci and H. V. Poor, "New trellis code design for spatial modulation", *IEEE Transactions on Wireless Communications*, Vol. 10, No. 8, pp. 2670–2680, 2011.

23. Yang, P., Y. L. Guan, Y. Xiao, M. Di Renzo, S. Li and L. Hanzo, "Transmit precoded spatial modulation: Maximizing the minimum Euclidean distance versus minimizing the bit error ratio", *IEEE Transactions on Wireless Communications*, Vol. 15, No. 3, pp. 2054–2068, 2016.

24. Yang, P., Y. Xiao, B. Zhang, M. El-Hajjar, S. Li and L. Hanzo, "Phase rotation-based precoding for spatial modulation systems", *IET Communications*, Vol. 9,

No. 10, pp. 1315–1323, 2015.

25. Masouros, C., "Improving the diversity of spatial modulation in MISO channels by phase alignment", *IEEE Communications Letters*, Vol. 18, No. 5, pp. 729–732, 2014.

26. Koca, M. and H. Sari, "Precoded Spatial Modulation for Robustness against Correlated Rician Fading", *GLOBECOM 2017-2017 IEEE Global Communications Conference*, pp. 1–6, IEEE, 2017.

27. Maharaj, B. T., L. P. Linde and J. W. Wallace, "MIMO Channel Modelling: the Kronecker model and maximum entropy", *Wireless Communications and Networking Conference, 2007. WCNC 2007. IEEE*, pp. 1909–1912, IEEE, 2007.

28. Zhou, B., Y. Xiao, P. Yang, J. Wang and S. Li, "Spatial modulation for single carrier wireless transmission systems", *Communications and Networking in China (CHINACOM), 2011 6th International ICST Conference on*, pp. 11–15, IEEE, 2011.

29. Liolis, K. P., J. Gómez-Vilardebó, E. Casini and A. I. Pérez-Neira, "Statistical modeling of dual-polarized MIMO land mobile satellite channels", *IEEE Transactions on Communications*, Vol. 58, No. 11, pp. 3077–3083, 2010.

30. Coldrey, M., "Modeling and capacity of polarized MIMO channels", *Vehicular Technology Conference, 2008. VTC Spring 2008. IEEE*, pp. 440–444, IEEE, 2008.

31. Oestges, C., B. Clerckx, M. Guillaud and M. Debbah, "Dual-polarized wireless communications: from propagation models to system performance evaluation", *IEEE Transactions on Wireless Communications*, Vol. 7, No. 10, 2008.

32. Erceg, V., P. Soma, D. S. Baum and A. J. Paulraj, "Capacity obtained from multiple-input multiple-output channel measurements in fixed wireless environments at 2.5 GHz", *Communications, 2002. ICC 2002. IEEE International Conference on*, Vol. 1, pp. 396–400, IEEE, 2002.

33. Lotse, F., J.-E. Berg, U. Forssen and P. Idahl, "Base station polarization diversity reception in macrocellular systems at 1800 MHz", *Vehicular Technology Conference, 1996. Mobile Technology for the Human Race., IEEE 46th*, Vol. 3, pp. 1643–1646, IEEE, 1996.

34. Asplund, H., J.-E. Berg, F. Harrysson, J. Medbo and M. Riback, "Propagation characteristics of polarized radio waves in cellular communications", *Vehicular Technology Conference, 2007. VTC-2007 Fall. 2007 IEEE 66th*, pp. 839–843, IEEE, 2007.

35. Nabar, R. U., H. Bolcskei, V. Erceg, D. Gesbert and A. J. Paulraj, "Performance of multiantenna signaling techniques in the presence of polarization diversity", *IEEE Transactions on Signal Processing*, Vol. 50, No. 10, pp. 2553–2562, 2002.

36. Clerckx, B., Y. Zhou and S. Kim, "Practical codebook design for limited feedback spatial multiplexing", *Communications, 2008. ICC'08. IEEE International Conference on*, pp. 3982–3987, IEEE, 2008.

37. Proakis, J. and M. Salehi, *Digital Communications*, Asia Higher Education Engineering/Computer Science Electrical Engineering, McGraw-Hill, 2008, `https://books.google.com.tr/books?id=ksh0GgAACAAJ`.

38. Basar, E., U. Aygolu, E. Panayirci and H. V. Poor, "Performance of spatial modulation in the presence of channel estimation errors", *IEEE Communications Letters*, Vol. 16, No. 2, pp. 176–179, 2012.

39. Di Renzo, M. and H. Haas, "A general framework for performance analysis of space shift keying (SSK) modulation for MISO correlated Nakagami-m fading channels", *IEEE Transactions on Communications*, Vol. 58, No. 9, pp. 2590–2603, 2010.

40. Koca, M. and H. Sari, "Performance of spatial modulation over correlated fading channels with channel estimation errors", *Wireless Communications and Networking Conference (WCNC), 2013 IEEE*, pp. 3937–3942, IEEE, 2013.

41. Borade, S., B. Nakiboglu and L. Zheng, "Unequal error protection: An information-

theoretic perspective", *IEEE Transactions on Information Theory*, Vol. 55, No. 12, pp. 5511–5539, 2009.